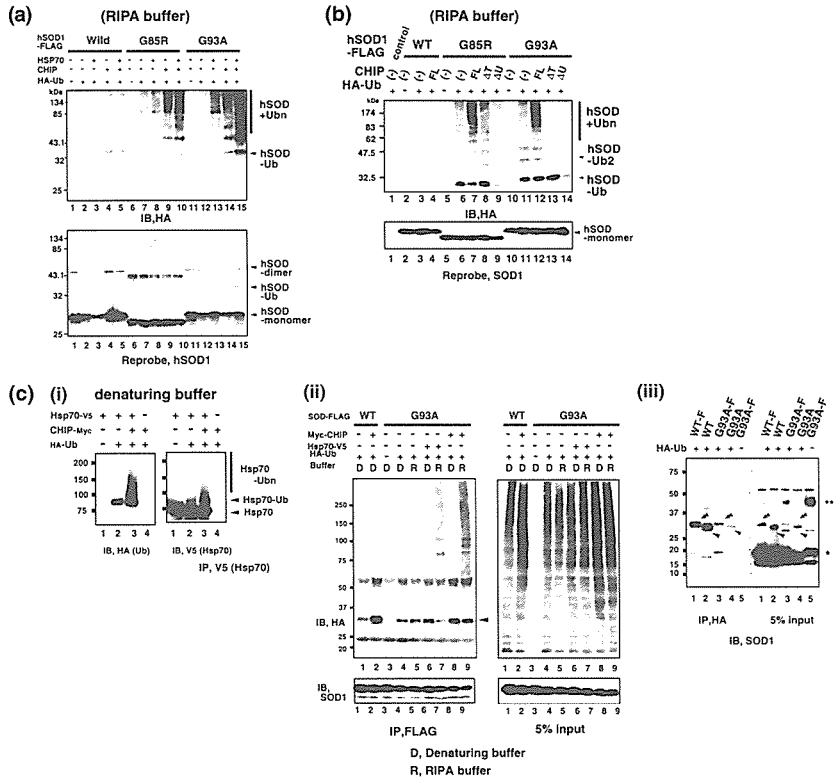

Fig. 3 CHIP does not target mutant SOD1, but ubiquitinates its interacting proteins. (a) Hsp70 and CHIP promoted formation of a complex consisting of hSOD1 and polyubiquitinated species, but did not covalently ubiquitinate SOD1 *in vivo*. Neuro2a cells in 6-well culture plates were transiently transfected with hSOD1-FLAG (1 μg/well), together with Hsp70-V5 (0.5 μg), Myc-CHIP (0.5 μg) or HA-Ub (total DNA, 2.5 μg/well). Cells were solubilized by RIPA buffer with sonication on ice, and lysates were immunoprecipitated in anti-FLAG affinity gel. Immunoprecipitates were incubated in 2% SDS sample buffer for 5 min at 95°C before resolving in 13% SDS-polyacrylamide gel (denaturing after immunoprecipitation). Blots were probed by anti-HA antibody and were reprobed by anti-SOD1 antibody. SOD1-Ub indicates monoubiquitinated SOD1. SOD-Ubn indicates complex of mutant SOD1 and polyubiquitinated species (does not necessarily mean covalently polyubiquitinated SOD1). (b) The effect of CHIP on the formation of the mutant SOD1-polyubiquitin complex required both TPR and U-box domains. Neuro2a cells in 6-well culture plates were transiently transfected with hSOD1-FLAG (1.5 μg), Myc-CHIP full-length (FL), deletion mutant of tetratricopeptide repeat domain (ΔTPR) or of U-box domain (ΔU; 0.5 μg), and HA-ubiquitin (HA-Ub; 0.5 μg) (total DNA, 2.5 μg/well). Immunoprecipitation and western analysis were performed in the same way as in (a). hSOD1-Ub_2 and -Ub indicate di and monoubiquitination of hSOD1, respectively. hSOD1 + Ubn indicates polyubiquitinated species associated with mutant hSOD1. (c) *In vivo* ubiquitination experiment showing polyubiquitin is not covalently bound to mutant SOD1. (1) *In vivo* ubiquitination using denaturing buffer showing Hsp70 is a substrate of CHIP. Neuro2a cells were transiently transfected with Hsp70-V5 and HA-ubiquitin (HA-Ub) with or without CHIP. Cells were solubilized by denaturing buffer containing 1% SDS buffer with boiling for 5 min. After diluting with a 10-fold volume of the dilution buffer, lysates were immunoprecipitated by anti-V5 antibody (denaturing before immunoprecipitation). Eluate was resolved in 5–20% gradient SDS polyacrylamide gel, and blots were probed by antibody against V5 or HA. Both panels indicate that Hsp70 is covalently bound to polyubiquitin in the presence of CHIP. (2) Mutant SOD1 is not a substrate of CHIP *in vivo*. Neuro2a cells were transiently transfected with hSOD1-FLAG, HA-Ub, Hsp70-V5 and Myc-CHIP as indicated. D indicates that cells were solubilized in denaturing buffer condition [samples were denatured before immunoprecipitation as in (1)], whereas R indicates that cells were solubilized in RIPA buffer condition [samples were denatured after immunoprecipitation as in (a) and (b)]. Immunoprecipitates and 5% input were resolved in 5–20% gradient SDS-polyacrylamide gel, and blots were probed by anti-HA or anti-SOD1 antibody. No significant elevation of ubiquitination was observed in lane 8 compared with 4, as in Fig. 3c (1). In denaturing buffer condition, only mono-ubiquitinated SOD1 in both wild-type and mutant was observed (arrowhead). (3) Both wild-type and mutant SOD1 are oligoubiquitinated. Neuro2a cells in 6-well plates were transfected with hSOD1 with or without FLAG tag (–F) and HA-Ub. Cell lysates in RIPA buffer were immunoprecipitated with anti-HA cross-linked beads and analyzed using antihSOD1 antibody.

et al. 2003). However, our data indicate that CHIP promotes the degradation of mutant SOD1 through a mechanism different from that for other CHIP substrates, such as glucocorticoid receptor (Connell *et al.* 2001), heat-denatured luciferase (Murata *et al.* 2001) and phosphorylated tau (Shimura *et al.* 2003).

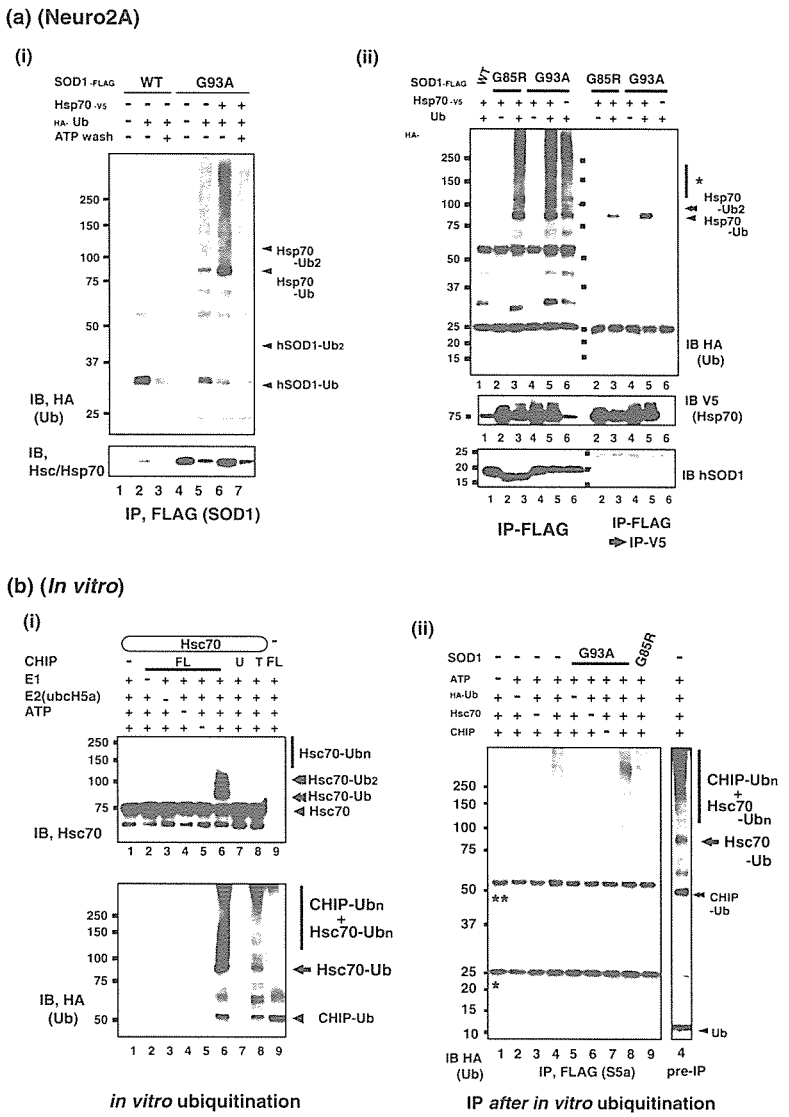

Fig. 4 Hsp/Hsc70 associated with mutant SOD1 is ubiquitinated. (a) Mutant SOD1-associated Hsp/Hsc70 polyubiquitinated *in vivo*. (1) Polyubiquitinated species were released from mutant SOD1 together with Hsp/Hsc70 by ATP wash *in vivo*. Neuro2a cells in 6-well plates were transfected with hSOD1-FLAG (1 μg/well) and HA-ubiquitin (HA-Ub, 1 μg/well) and solubilized in RIPA buffer with sonication. Lysates were immunoprecipitated by anti-FLAG affinity gel. Immunoprecipitates were washed in the buffer containing 10 mM ATP and 5 mM $MgCl_2$ for 15 min at 37°C. Eluates were resolved in 5–20% gradient SDS-polyacrylamide gel, and blots were probed by anti-HA and anti-Hsp/Hsc70 antibodies. (2) Mutant SOD1-associated Hsp70 was ubiquitinated. Neuro2a cells were transfected with hSOD1-FLAG, Hsp70-V5 and HA-ubiquitin. Cells were solubilized in RIPA buffer with sonication and the supernatant fluid was immunoprecipitated by anti-FLAG affinity gel. Half of the immunoprecipitates were eluted by 2% SDS-sample buffer with boiling, and the rest were sequentially immunoprecipitated by anti-V5 antibody (see Experimental procedures). The eluates from the first and second immunoprecipitates were resolved in 5–20% gradient SDS polyacrylamide gel, and the blot was probed by anti-HA antibody. (b) Polyubiquitinated Hsc70 associated with the S5a subunit of the 26S proteasome. (1) *In vitro* ubiquitination experiments demonstrating that CHIP ubiquitinated Hsc70 in the presence of E1, E2 and ATP. CHIP also ubiquitinated itself (auto-ubiquitination) as shown by the blot probed by anti-HA antibody (lower panel). The reaction mixture was resolved in 5–20% gradient SDS-polyacrylamide gel, and the blot was probed with anti-HA or anti-Hsp/Hsc70 antibody. (2) After *in vitro* ubiquitination reaction with or without SOD1 protein as in (1), reaction mixtures were incubated with FLAG-tagged recombinant S5a protein and immunolinked to anti-FLAG affinity gel. The reaction mixture was resolved in 5–20% gradient SDS-polyacrylamide gel, and the blot was probed with anti-HA or anti-Hsp/Hsc70 antibody. The sample from lane 4 was loaded as a control without immunoprecipitation. The asterisk indicates IgG light chain, whereas double asterisks indicate IgG heavy chain.

We initially expected CHIP to ubiquitinate mutant SOD1, and CHIP did promote the formation of mutant SOD1-polyubiquitin complex (Fig. 3a). However, mutant SOD1 is not covalently polyubiquitinated, while its binding partner, including Hsp/Hsc70, was linked to polyubiquitin by covalent bond [Figs 3c (2) and 4a]. Taken with the finding that polyubiquitinated species containing Hsc70 associate with the S5a subunit of the 26S proteasome, it is plausible that ubiquitinated Hsp/Hsc70 accompanies mutant SOD1 to the 26S proteasome. However, it is still unclear how mutant SOD1, without a polyubiquitin chain, degrades at the 26S proteasome. Several oxidized proteins are reportedly degraded at the 20S proteasome in an ATP- or ubiquitin-independent manner (Ferrington *et al.* 2001; Shringarpure *et al.* 2003), which is a possible explanation for proteasomal degradation of mutant SOD1 since SOD1 itself is modified by oxidation (Andrus *et al.* 1998; Urushitani *et al.* 2002). An alternative explanation may be that a co-chaperone, BAG-1, might play a role in recruiting mutant SOD1 at the proteasome, since BAG-1 accepts substrate proteins from Hsp/Hsc70 and promotes CHIP-induced degradation (Demand *et al.* 2001; Alberti *et al.* 2002). Our data indicate that interaction with Hsp/Hsc70 determines the degradation fate of mutant SOD1. Recent findings that cultured motor neurons have limited Hsp70 expression (Bruening *et al.* 1999) and promoter activity (Batulan *et al.* 2003) suggest that insufficient proteasomal degradation of mutant SOD1 may lead to aggregate formation in motor neurons.

Molecular features of mutant SOD1-ubiquitin complex

From the *in vivo* ubiquitination study under the denaturing condition, it is shown that both wild-type and mutant SOD1 are oligoubiquitinated (Fig. 3b, 2 and 3). Moreover, we observed no overt polyubiquitination product of mutant SOD1 in a series of *in vitro* and *in vivo* ubiquitination experiments using S100 lysates from HeLa cells, HEK293T cells and Neuro2a cells (data not shown). Because mutant SOD1 readily aggregates or fragments (Urushitani *et al.* 2002), it is sometimes difficult to clearly differentiate the oligoubiquitination of aggregated SOD1 from the polyubiquitinated form. Although the physiological function of oligoubiquitination of SOD1 is unknown, it is unlikely that this is the signal for proteasomal degradation. However, it is still possible that there might be other ubiquitin chain elongation factors, namely E4, that recognize oligoubiquitinated species (Koegl *et al.* 1999), and a chaperone-associated E4 may explain the difference between wild-type and mutants. Furthermore, other ubiquitin ligases, such as dorfin (Niwa *et al.* 2002), may co-operate with chaperone-CHIP machineries. Nevertheless, our data indicate that the mutant SOD1-polyubiquitin complex is composed of various polyubiquitinated species including Hsp70 and/or CHIP. Immunohistochemical analysis revealed that Lewy body-like hyaline inclusions (LBHIs) in the remaining motor neurons

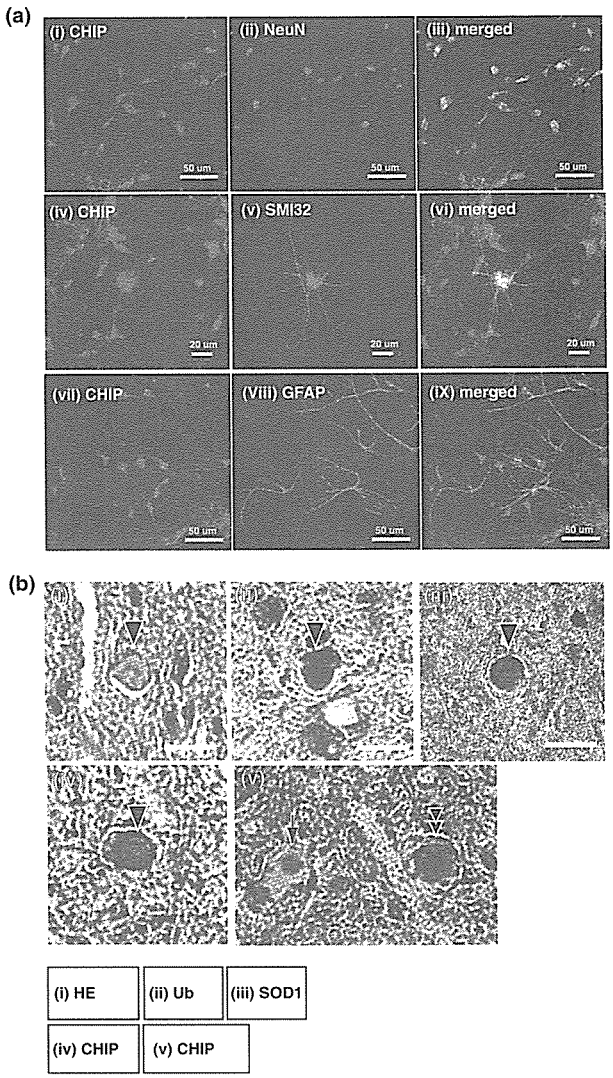

Fig. 5 CHIP is expressed abundantly in neurons, and Lewy body-like hyaline inclusions (LBHIs) are CHIP-immunoreactive. (a) CHIP is expressed predominantly in neurons including motor neurons of embryonic spinal cord cultures (E12). Dissociated cultures at 8 days after plating were fixed and doubly-stained by CHIP (1, 4, 7) and various cell markers (2, anti-NeuN; 5, anti-non-phosphorylated neurofilament H (SMI32); 8, anti-GFAP antibodies, respectively). 3, 8, and 9 are merged images from 1–2, 4–5 and 7–8, respectively. (b) CHIP-immunoreactive Lewy body-like hyaline inclusions (LBHI) in the spinal cord of a 180-day-old hSOD1^{G93A} transgenic mouse. Panel 1 shows a typical LBHI with eosinophilic structure in hematoxylin-eosin (H&E) preparation. Panels 2, 3 and 4 exhibit immunostaining of ubiquitin, mutant SOD1 and CHIP, respectively. In panel 5, various CHIP staining patterns are seen in LBHIs: core-staining (arrow) and diffuse-staining (arrowheads) patterns. Panels 1–5 are × 400 and 2–5 are weakly counterstained with hematoxylin. Scale bar, 20 μm.

of hSOD1^{G93A} transgenic mice were CHIP immunoreactive (Fig. 5b). These aggregates are highly Hsc70-immunoreactive (Watanabe *et al.* 2001), which, together with our

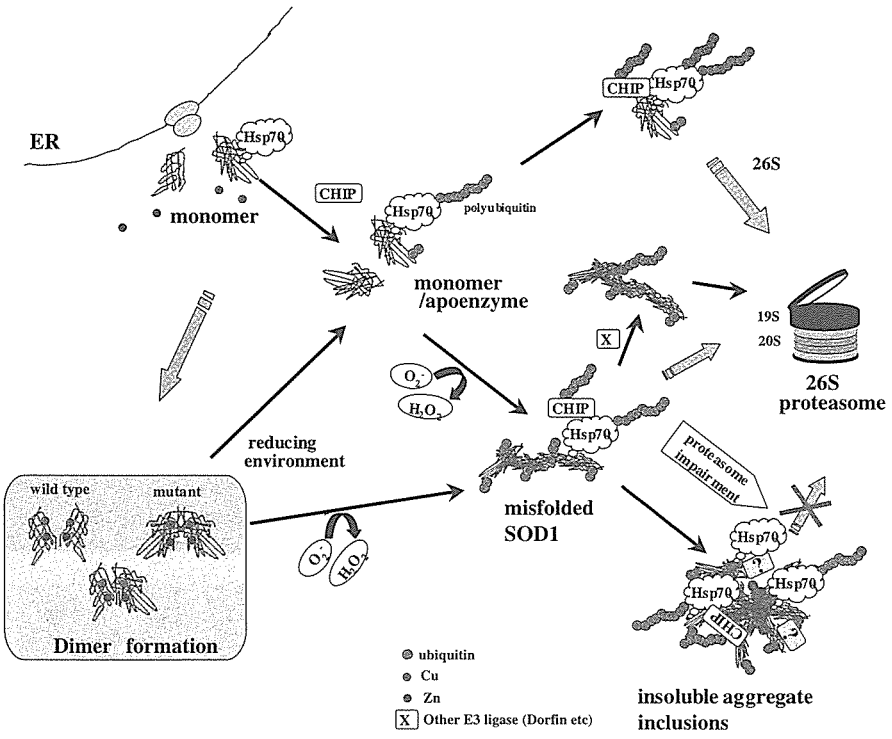

Fig. 6 Hypothetical mechanism for mutant SOD1 degradation. The nascent monomeric SOD1 before metallation in both wild-type and mutant may be bound to Hsp/Hsc70 for folding into the proper conformation. In the mutants, a considerable amount of SOD1 may not fold properly and may remain as a monomer. In the course of this process, Hsp/Hsc70 might be polyubiquitinated by CHIP and recruited to the 26S proteasome. Even in the dimeric forms, mutant SOD1 is susceptible to reducing conditions, resulting in a monomer, which may be recognized by Hsp/Hsc70. The oxidative stress augmented the abnormal conformation of mutant SOD1, and the proteasomal impairment under these conditions may result in the observed pathological ubiquitin-positive aggregation.

findings, suggests the involvement of Hsp/Hsc70-CHIP machinery in the metabolism of mutant SOD1 in the ALS mouse model containing mutant SOD1. Although we showed that CHIP was expressed predominantly in the neurons, including motor neurons of the spinal cord, western analysis of the primary astrocyte culture revealed that CHIP was also expressed in astrocytes (data not shown). In this regard, it would be interesting to examine whether CHIP is localized to the glial LBHIs in $hSOD1^{G85R}$ transgenic mice and some human ALS cases (Bruijn *et al.* 1997; Kato *et al.* 1997). We have also observed that CHIP and Hsp/Hsc70 accumulate in insoluble fractions of the spinal cord lysates from mutant SOD1 transgenic mice as ALS progresses (unpublished observation). However, this is not transcriptionally regulated because the mRNA profile analyzed by TaqMan chemistry provided no significant alteration in CHIP expression patterns in motor neurons with respect to the disease course (data not shown).

In conclusion, we have provided evidence that proteasomal translocation of mutant SOD1 is regulated by the ubiquitination of Hsp/Hsc 70. Currently, it is widely accepted that neurodegenerative diseases, including Alzheimer's disease, Parkinson's disease and polyglutamine disease, are caused by the accumulation of misfolded proteins in neurons. Such aberrant proteins may be degraded in a similar manner, considering the interaction of Hsp/Hsc70 with disease-causing proteins.

Acknowledgements

We thank Dr Hidemi Misawa (Tokyo Metropolitan Institute for Neuroscience) for helpful discussions, and Dr Yuzuru Imai and Ms Mariko Soda for providing anti-CHIP antibody and constructs for Hsp70. We also thank Dr Yasuyuki Suzuki for his cooperation with our experiment, and for his generous gift of recombinant XIAP and Smac proteins. We also thank Dr Kazuhiro Yamanaka (Ludwig Institute for Cancer Research, San Diego, USA) for his critical advice on the *in vitro* ubiquitination assay. This work was supported by research grants from RIKEN BSI, a Grant-in-Aid from the Japan Society for the Promotion of Science (JSPS), a Grant-in-Aid from the Japan Foundation for Neuroscience and Mental Health, and by grants from the Ministry of Health and Welfare, Japan.

References

Abernethy J. L., Steinman H. M. and Hill R. L. (1974) Bovine erythrocyte superoxide dismutase. Subunit structure and sequence

location of the intrasubunit disulfide bond. *J. Biol. Chem.* **249**, 7339–7347.

Adachi H., Katsuno M., Minamiyama M. *et al.* (2003) Heat shock protein 70 chaperone overexpression ameliorates phenotypes of the spinal and bulbar muscular atrophy transgenic mouse model by reducing nuclear-localized mutant androgen receptor protein. *J. Neurosci.* **23**, 2203–2211.

Alberti S., Demand J., Esser C., Emmerich N., Schild H. and Hohfeld J. (2002) Ubiquitylation of BAG-1 suggests a novel regulatory mechanism during the sorting of chaperone substrates to the proteasome. *J. Biol. Chem.* **277**, 45920–45927.

Andrus P. K., Fleck T. J., Gurney M. E. and Hall E. D. (1998) Protein oxidative damage in a transgenic mouse model of familial amyotrophic lateral sclerosis. *J. Neurochem.* **71**, 2041–2048.

Aravind L. and Koonin E. V. (2000) The U box is a modified RING finger – a common domain in ubiquitination. *Curr. Biol.* **10**, R132–R134.

Bailey C. K., Andriola I. F., Kampinga H. H. and Merry D. E. (2002) Molecular chaperones enhance the degradation of expanded polyglutamine repeat androgen receptor in a cellular model of spinal and bulbar muscular atrophy. *Hum. Mol. Genet.* **11**, 515–523.

Ballinger C. A., Connel P., Wu Y., Thompson L. J., Yin L. Y. and Patterson C. (1999) Identification of CHIP, a novel tetratricopeptide repeat-containing protein that interacts with heat shock proteins and negatively regulates chaperone functions. *Mol. Cell. Biol.* **19**, 4535–4545.

Bartnikas T. B. and Gitlin J. D. (2003) Mechanisms of biosynthesis of mammalian copper/zinc superoxide dismutase. *J. Biol. Chem.* **278**, 33602–33608.

Batulan Z., Shinder G. A., Minotti S., He B. P., Doroudchi M. M., Nalbantoglu J., Strong M. J. and Durham H. D. (2003) High threshold for induction of the stress response in motor neurons is associated with failure to activate HSF1. *J. Neurosci.* **23**, 5789–5798.

Bercovich B., Stancovski I., Mayer A., Blumenfeld N., Laszlo A., Schwartz A. L. and Ciechanover A. (1997) Ubiquitin-dependent degradation of certain protein substrates in vitro requires the molecular chaperone Hsc70. *J. Biol. Chem.* **272**, 9002–9010.

Bruening W., Roy J., Giasson B., Figlewicz D. A., Mushynski W. E. and Durham H. D. (1999) Up-regulation of protein chaperones preserves viability of cells expressing toxic Cu/Zn-superoxide dismutase mutants associated with amyotrophic lateral sclerosis. *J. Neurochem.* **72**, 693–699.

Bruijn L. I., Becher M. W., Lee M. K. *et al.* (1997) ALS-linked SOD1 mutant G85R mediates damage to astrocytes and promotes rapidly progressive disease with SOD1-containing inclusions. *Neuron* **18**, 327–338.

Cardozo C. P., Michaud C., Ost M. C., Fliss A. E., Yang E., Patterson C., Hall S. J. and Caplan A. J. (2003) C-terminal Hsp-interacting protein slows androgen receptor synthesis and reduces its rate of degradation. *Arch. Biochem. Biophys.* **410**, 134–140.

Cleveland D. W. and Rothstein J. D. (2001) From Charcot to Lou Gehrig: deciphering selective motor neuron death in ALS. *Nat. Rev. Neurosci.* **2**, 806–819.

Connell P., Ballinger C. A., Jiang J., Wu Y., Thompson L. J., Hohfeld J. and Patterson C. (2001) The co-chaperone CHIP regulates protein triage decisions mediated by heat-shock proteins. *Nat. Cell Biol.* **3**, 93–96.

Demand J., Alberti S., Patterson C. and Hohfeld J. (2001) Cooperation of a ubiquitin domain protein and an E3 ubiquitin ligase during chaperone/proteasome coupling. *Curr. Biol.* **11**, 1569–1577.

Elam J. S., Taylor A. B., Strange R. *et al.* (2003) Amyloid-like filaments and water-filled nanotubes formed by SOD1 mutant proteins linked to familial ALS. *Nat. Struct. Biol.* **10**, 461–467.

Ferrington D. A., Sun H., Murray K. K., Costa J., Williams T. D., Bigelow D. J. and Squier T. C. (2001) Selective degradation of oxidized calmodulin by the 20 S proteasome. *J. Biol. Chem.* **276**, 937–943.

Gurney M. E., Pu H., Chiu A. Y., Dal Canto M. C., Polchow C. Y., Alexander D. D., Caliendo J., Hentati A., Kwon Y. W. and Deng H. X. (1994) Motor neuron degeneration in mice that express a human Cu, Zn superoxide dismutase mutation. *Science* **264**, 1772–1775.

Hatakeyama S., Yada M., Matsumoto M., Ishida N. and Nakayama K. (2001) U box proteins as a new family of ubiquitin-protein ligases. *J. Biol. Chem.* **276**, 33111–33120.

Imai Y., Soda M., Hatakeyama S., Akagi T., Hashikawa T., Nakayama K. I. and Takahashi R. (2002) CHIP is associated with Parkin, a gene responsible for familial Parkinson's disease, and enhances its ubiquitin ligase activity. *Mol. Cell* **10**, 55–67.

Jiang J., Ballinger C. A., Wu Y., Dai Q., Cyr D. M., Hohfeld J. and Patterson C. (2001) CHIP is a U-box-dependent E3 ubiquitin ligase: identification of Hsc70 as a target for ubiquitylation. *J. Biol. Chem.* **276**, 42938–42944.

Johnston J. A., Dalton M. J., Gurney M. E. and Kopito R. R. (2000) Formation of high molecular weight complexes of mutant Cu, Zn-superoxide dismutase in a mouse model for familial amyotrophic lateral sclerosis. *Proc. Natl Acad. Sci. USA* **97**, 12571–12576.

Julien J. P. (2001) Amyotrophic lateral sclerosis. Unfolding the toxicity of the misfolded. *Cell* **104**, 581–591.

Kang J. H. and Eum W. S. (2000) Enhanced oxidative damage by the familial amyotrophic lateral sclerosis-associated Cu, Zn-superoxide dismutase mutants. *Biochim. Biophys. Acta* **1524**, 162–170.

Kato S., Hayashi H., Nakashima K., Nanba E., Kato M., Hirano A., Nakano I., Asayama K. and Ohama E. (1997) Pathological characterization of astrocytic hyaline inclusions in familial amyotrophic lateral sclerosis. *Am. J. Pathol.* **151**, 611–620.

Koegl M., Hoppe T., Schlenker S., Ulrich H. D., Mayer T. U. and Jentsch S. (1999) A novel ubiquitination factor, E4, is involved in multiubiquitin chain assembly. *Cell* **96**, 635–644.

Lindberg M. J., Tibell L. and Oliveberg M. (2002) Common denominator of Cu/Zn superoxide dismutase mutants associated with amyotrophic lateral sclerosis: decreased stability of the apo state. *Proc. Natl Acad. Sci. USA* **99**, 16607–16612.

Meacham G. C., Patterson C., Zhang W., Younger J. M. and Cyr D. M. (2001) The Hsc70 co-chaperone CHIP targets immature CFTR for proteasomal degradation. *Nat. Cell Biol.* **3**, 100–105.

Murata S., Minami Y., Minami M., Chiba T. and Tanaka K. (2001) CHIP is a chaperone-dependent E3 ligase that ubiquitylates unfolded protein. *EMBO Rep.* **2**, 1133–1138.

Nakano R., Inuzuka T., Kikugawa K., Takahashi H., Sakimura K., Fujii J., Taniguchi N. and Tsuji S. (1996) Instability of mutant Cu/Zn superoxide dismutase (Ala4Thr) associated with familial amyotrophic lateral sclerosis. *Neurosci. Lett.* **211**, 129–131.

Niwa J., Ishigaki S., Hishikawa N., Yamamoto M., Doyu M., Murata S., Tanaka K., Taniguchi N. and Sobue G. (2002) Dorfin ubiquitylates mutant SOD1 and prevents mutant SOD1-mediated neurotoxicity. *J. Biol. Chem.* **277**, 36793–36798.

van Nocker S., Deveraux Q., Rechsteiner M. and Vierstra R. D. (1996) Arabidopsis MBP1 gene encodes a conserved ubiquitin recognition component of the 26S proteasome. *Proc. Natl Acad. Sci. USA* **93**, 856–860.

Okado-Matsumoto A. and Fridovich I. (2002) Amyotrophic lateral sclerosis: a proposed mechanism. *Proc. Natl Acad. Sci. USA* **99**, 9010–9014.

Rosen D. R., Siddique T., Patterson D. *et al.* (1993) Mutations in Cu/Zn superoxide dismutase gene are associated with familial amyotrophic lateral sclerosis. *Nature* **362**, 59–62.

Shimura H., Schwartz D., Gygi S. P. and Kosik K. S. (2003) CHIP-Hsc70 complex ubiquitinates phosphorylated Tau and enhances cell survival. *J. Biol. Chem.* **279**, 4869–4876.

Shinder G. A., Lacourse M. C., Minotti S. and Durham H. D. (2001) Mutant Cu/Zn-superoxide dismutase proteins have altered solubility and interact with heat shock/stress proteins in models of amyotrophic lateral sclerosis. *J. Biol. Chem.* **276**, 12791–12796.

Shringarpure R., Grune T., Mehlhase J. and Davies K. J. (2003) Ubiquitin conjugation is not required for the degradation of oxidized proteins by proteasome. *J. Biol. Chem.* **278**, 311–318.

Strange R. W., Antonyuk S., Hough M. A., Doucette P. A., Rodriguez J. A., Hart P. J., Hayward L. J., Valentine J. S. and Hasnain S. S. (2003) The structure of holo and metal-deficient wild-type human Cu, Zn superoxide dismutase and its relevance to familial amyotrophic lateral sclerosis. *J. Mol. Biol.* **328**, 877–891.

Tiwari A. and Hayward L. J. (2003) Familial amyotrophic lateral sclerosis mutants of copper/zinc superoxide dismutase are susceptible to disulfide reduction. *J. Biol. Chem.* **278**, 5984–5992.

Urushitani M., Kurisu J., Tsukita K. and Takahashi R. (2002) Proteasomal inhibition by misfolded mutant superoxide dismutase 1 induces selective motor neuron death in familial amyotrophic lateral sclerosis. *J. Neurochem.* **83**, 1030–1042.

Valentine J. S. and Hart P. J. (2003) Misfolded CuZnSOD and amyotrophic lateral sclerosis. *Proc. Natl Acad. Sci. USA* **100**, 3617–3622.

Walters K. J., Kleijnen M. F., Goh A. M., Wagner G. and Howley P. M. (2002) Structural studies of the interaction between ubiquitin family proteins and proteasome subunit S5a. *Biochemistry* **41**, 1767–1777.

Watanabe M., Dykes-Hoberg M., Culotta V. C., Price D. L., Wong P. C. and Rothstein J. D. (2001) Histological evidence of protein aggregation in mutant SOD1 transgenic mice and in amyotrophic lateral sclerosis neural tissues. *Neurobiol. Dis.* **8**, 933–941.

Xu W., Marcu M., Yuan X., Mimnaugh E., Patterson C. and Neckers L. (2002) Chaperone-dependent E3 ubiquitin ligase CHIP mediates a degradative pathway for c-ErbB2/Neu. *Proc. Natl Acad. Sci. USA* **99**, 12847–12852.

[CANCER RESEARCH 64, 3452–3457, May 15, 2004]

Antiapoptotic Function of Apoptosis Inhibitor 2-MALT1 Fusion Protein Involved in t(11;18)(q21;q21) Mucosa-Associated Lymphoid Tissue Lymphoma

Yoshitaka Hosokawa,[1] Hiroko Suzuki,[1] Yasuyuki Suzuki,[2] Ryosuke Takahashi,[2] and Masao Seto[1]

[1]Division of Molecular Medicine, Aichi Cancer Center Research Institute, Nagoya, Japan, and [2]Laboratory for Motor System Neurodegeneration, RIKEN Brain Science Institute, Wako City, Saitama, Japan

ABSTRACT

t(11;18)(q21;q21) is a characteristic chromosomal translocation in mucosa-associated lymphoid tissue (MALT) type lymphoma, and this translocation results in fusion transcript of *apoptosis inhibitor 2* (*API2*), also known as *c-IAP2*, and *MALT translocation* gene 1 (*MALT1*). Although the API2-MALT1 fusion protein has been shown to enforce activation of nuclear factor κB signaling, its precise role in the apoptotic signaling pathway remains to be established. To identify proteins that bind the API2-MALT1 protein, we used coimmunoprecipitation and SDS-PAGE, followed by liquid chromatography-electrospray ionization tandem mass spectrometry. As a result, three important regulators of apoptosis, Smac, HtrA2, and TRAF2, and three other proteins were identified as potential API2-MALT1-binding proteins. Immunoprecipitation analyses verified that API2-MALT1 indeed binds to both exogeneous and endogeneous Smac proteins. It is especially noteworthy that stably transfected API2-MALT1 significantly suppressed both UV- and etoposide-induced apoptosis in HeLa cells, thus demonstrating for the first time that API2-MALT1 indeed possesses antiapoptotic function. Furthermore, API2-MALT1 significantly suppressed Smac-promoted apoptosis in UV-irradiated HeLa cells. Thus, our results provide direct experimental evidence that API2-MALT1 can confer resistance to apoptosis, at least in part, by neutralizing apoptosis promoted by Smac.

INTRODUCTION

Extranodal lymphomas arising from the mucosa-associated lymphoid tissue (MALT) represent a subtype of B-cell non-Hodgkin's lymphoma with a distinct clinicopathological entity (1). Because of their supposed cell of origin, they are now recognized and defined as extranodal marginal zone lymphomas of MALT type in the revised European-American classification of lymphoid neoplasms (REAL) and the recently published WHO classification of malignant lymphomas (2, 3). According to the International Non-Hodgkin's Lymphoma Classification Project, MALT lymphoma comprises 7.6% of all non-Hodgkin's lymphomas and represents one of the most common non-Hodgkin's lymphomas (4). The majority of MALT lymphomas occur in the stomach, but this lymphoma may affect most organs, including the ocular adnexa, lung, salivary glands, thyroid, skin, and intestine.

Data on the molecular genetic mechanisms underlying the pathogenesis of MALT lymphomas are only now beginning to emerge. Their recurrent abnormalities include trisomies of chromosomes 3, 7, 12, and 18, t(1;14)(p22;q32), and t(11;18)(q21;q21) (5–9). The *BCL10* gene was isolated from the breakpoint region of the t(1;14) in MALT lymphomas and subsequently shown to be proapoptotic (10, 11). On the other hand, the t(11;18) translocation is reported to be one of the most frequent and specific chromosomal translocations in MALT lymphomas (12), and a novel gene, named *MALT1* or *MLT*, was recently cloned by ourselves and others from the breakpoint of t(11;18). This aberration has been found to result in the fusion of two genes, *apoptosis inhibitor 2* [*API2* (also known as *c-IAP2*)] at 11q21 and the novel gene *MALT1* at 18q21 (13–15), generating the API2-MALT1 fusion protein. More recently, a novel t(14;18) translocation involving the immunoglobulin gene at 14q32 and the *MALT1* gene at 18q21 has been reported (16, 17), and the actual frequency of this translocation in MALT lymphoma is roughly 10% (18, 19).

API2 is a member of the inhibitor of apoptosis (*IAP*) protein gene family, which includes *X-IAP, API1 (c-IAP1), API2 (c-IAP2)*, and *ML-IAP*, and has three baculovirus IAP repeat domains, one caspase recruitment domain, and one RING finger domain (20, 21). MALT1 is a novel protein that contains a death domain, two immunoglobulin-like domains, and a caspase-like domain (13–15, 22). It was demonstrated that MALT1 and BCL10 form a strong complex and that these proteins synergize in nuclear factor (NF)-κB activity (22, 23). Together with the findings for *BCL10* and *MALT1* knockout mice, these results suggest that both MALT1 and BCL10 link antigen receptor signaling to NF-κB activation (24–26). The caspase-like domain of MALT1 was demonstrated to be essential for NF-κB activity (22, 23), but functions of the death domain and immunoglobulin-like domains remain to be identified. It was also demonstrated that API2-MALT1 can induce NF-κB activation through its homodimerization mediated via the API2 portion of the fusion protein, whereas full-length API2, MALT, or their truncated forms cannot (22, 23), raising the possibility that the oncogenic role of API2-MALT1 may be mediated by deregulated NF-κB activity. Given that API2 is a member of the IAP family, it can be hypothesized that API2-MALT1 may exert an antiapoptotic effect as well. However, experimental evidence for such an antiapoptotic effect has yet to be presented.

In this study, we first tried to identify the binding proteins of API2-MALT1 to further delineate its apoptotic and oncogenic functions. To this end, we used electrospray ionization tandem mass spectrometry analysis of the coimmunoprecipitates of transiently transfected API2-MALT1 in cultured cells and were able to identify Smac (27, 28) as consisting of several API2-MALT1-binding proteins. We also demonstrated for the first time that API2-MALT1 can significantly suppress both UV- and etoposide-induced apoptosis in HeLa cells and that this suppression may be mediated, at least in part, by neutralizing apoptosis promoted by Smac.

MATERIALS AND METHODS

Plasmids and Antibodies. The plasmids encoding FLAG-API2-MALT1 (pcDNA3-FLAG-API2-MALT1 and PCXN2-FLAG-API2-MALT1) have been described elsewhere (29), as has the plasmid for COOH-terminal myc-tagged Smac (pcDNA3-Smac-myc) (30). To generate the plasmids for pRK5-FLAG-API2ΔC (amino acids 1–442) and pRK5-FLAG-MALT1ΔN (amino acids 217–813), the corresponding fragments were PCR amplified using KOD Taq polymerase from their full-length cDNAs, digested with the appropriate enzymes, and then subcloned into pRK5-FLAG-N plasmids. Proper construction of these plasmids was confirmed by DNA sequencing with the ABI PRISM BigDye Terminator Cycle Sequencing Ready Reaction kit (Perkin-Elmer, Foster City, CA). The pEGFP-C plas-

Received 11/25/03; revised 2/16/04; accepted 3/5/04.

Grant support: A Grant-in-Aid for the Second Term Comprehensive 10-Year Strategy for Cancer Control from the Ministry of Health and Welfare and a Grant-in-Aid for Science in Primary Areas (Cancer Research) from the Ministry of Education, Science, Sports and Culture, Japan.

The costs of publication of this article were defrayed in part by the payment of page charges. This article must therefore be hereby marked *advertisement* in accordance with 18 U.S.C. Section 1734 solely to indicate this fact.

Requests for reprints: Yoshitaka Hosokawa, Division of Molecular Medicine, Aichi Cancer Center Research Institute, 1-1 Kanokoden, Chikusa-ku, Nagoya 464-8681, Japan. Phone: 81-52-762-6111, ext.7083; Fax: 81-52-763-5233; E-mail: yhosokaw@aichi-cc.jp.

mid was purchased from Clontech. Anti-FLAG M2 monoclonal antibody and polyclonal antibody against myc (A-14) were obtained from Santa Cruz Biotechnology. Anti-FLAG monoclonal antibody-coupled agarose beads were obtained from Sigma (St. Louis, MO).

Purification of API2-MALT1-Binding Proteins. 293T cells were maintained in Iscove's medium supplemented with 10% FCS in a 5% CO_2 incubator at 37°C. The pcDNA3 FLAG-tagged API2-MALT1 plasmid or the empty plasmid was transiently transfected into 293T cells using Effectene Reagent (Qiagen K.K., Tokyo, Japan) according to the manufacturer's instructions. At 24 h after transfection, the cells were homogenized in lysis buffer [10 mM Tris (pH 8.0), 120 mM NaCl, 5 mM EDTA, and 0.5% Triton X-100] with Complete Protease Inhibitors (Roche Diagnostics, Tokyo, Japan). The homogenate was centrifuged twice at 10,000 × g for 15 min. The soluble fraction of the suspension was then incubated for 3 h, immunoprecipitated with anti-FLAG M2-agarose beads (Sigma), and washed five times in lysis buffer without protease inhibitors. The fractions eluted with 0.2 M glycine-HCl (pH 2.8) were neutralized, concentrated by freeze drying, and separated by 10% SDS-PAGE (15 × 15 cm). The bands detected by Coomassie Brilliant Blue staining were excised for in-gel digestion.

High-Performance Liquid Chromatography Tandem Mass Spectrometry Analysis. In-gel digestion was performed by trypsin digestion at 35°C overnight as described elsewhere (31). The digest was analyzed directly by means of nanoscale high-performance liquid chromatography coupled to a tandem mass spectrometer (Q-Tof2; Micromass) equipped with a nanoelectrospray ionization source. The eluate was analyzed by tandem mass spectrometry (Q-Tof2) performed by Applied Bioscience (Tokushima, Japan). A database search of tandem mass spectra was performed using a Mascot Search Program (Matrix Science Ltd., London, United Kingdom).

Immunoprecipitation and Western Blot Analysis. 293T cells were transiently transfected using Effectene Reagent (Qiagen K.K.) or LipofectAMINE 2000 reagent (GIBCO-BRL, Tokyo, Japan) according to the manufacturer's instructions. For immunoprecipitation, a total of 8×10^5 293T cells were placed on a 3.5-cm dish or a 6-well dish, washed the following day, and then transfected with a total of 0.5–1.0 μg of plasmid DNA. After 6 h of incubation, the medium was replaced with fresh complete medium. At 24 h after transfection, the cells were homogenized in lysis buffer [20 mM HEPES (pH 7.4), 120 mM NaCl, 5 mM EDTA, 0.5% Triton X-100, and 10% glycerol] with Complete Protease Inhibitors (Roche Diagnostics). Cellular debris was removed by centrifugation at 10,000 × g for 20 min, and the supernatant was incubated first with anti-FLAG monoclonal antibody at 4°C for 2 h and then with protein G-Sepharose at 4°C for 2 h. Immunoprecipitates were washed five times in lysis buffer without protease inhibitors. After this, immunoprecipitates were lysed with 1× sample buffer [62.5 mM Tris-HCl (pH 6.8), 2% SDS, 10% glycerol, 5% mercaptoethanol, and 0.05% bromphenol blue] and boiled for 3 min. It should be noted that the lysis buffer solubilizes mitochondrial membranes and thus releases Smac without the need for any apoptotic stimuli.

The samples were separated electrophoretically on SDS-PAGE and transferred to a polyvinylidene difluoride membrane, and the membrane was visualized with an enhanced chemiluminescence detection kit (Amersham-Japan, Tokyo, Japan).

Establishment of Stable Transfectants Expressing API2-MALT1. The linearized pCXN2-FLAG-tagged API2-MALT or the control pCXN2 plasmid was transfected into HeLa cells using LipofectAMINE 2000 reagent (GIBCO-BRL) according to the manufacturer's instructions. At 24 h after transfection, the cells were seeded in several dilutions. At 48 h after transfection, Geneticin (IBL, Fujioka, Japan) was added to the medium at a final concentration of 1 mg/ml. This was then diluted over subsequent days by adding fresh medium. On the seventh day, Geneticin was diluted to a final concentration of 100 μg/ml. The surviving cells were grown for 1 more week and analyzed by Western blot analysis using an anti-FLAG monoclonal antibody for API2-MALT protein expression. One part of the cell population was seeded into 96-well plates at a density of 0.3 cells/well and propagated at 100 μg/ml Geneticin. The surviving colonies were again analyzed by Western blot analysis for API2-MALT1 protein expression. Two independent clones expressing API2-MALT1 were selected for further study. The two clones were maintained in Iscove's medium supplemented with 10% FCS and 500 μg/ml Geneticin.

Cell Death Assay. Stable transfectants with or without API2-MALT1 expression were seeded at 3×10^5 cells/3.5-cm dish in Iscove's medium supplemented with 10% FCS but without Geneticin. After 24 h, the medium was removed, and the cells were exposed to UV irradiation (200 J/m^2) with Stratalinker UV cross-linker 1800 (Stratagene, La Jolla, CA). The UV-treated cells were then cultured in fresh medium for 6 h. The transfectants were also treated with etoposide (100 μM) or DMSO for 12 h. Apoptosis was assessed by determining the percentages of cells that had condensed chromatin detected by staining with Hoechst 33342 (1 μg/ml) in serum-free medium for 10 min after fixation with 4% paraformaldehyde. At least 100 chromatins were counted in every sample.

For the apoptosis assay of HeLa cells transiently transfected with Smac-myc vector, the stable transfectant cells were transiently transfected with 0.5 μg of pEGFP-C plasmid (Clontech) plus either 2 μg of pcDNA3-Smac-myc or 2 μg of pcDNA3 plasmid control per dish. At 6 h after transfection, the cells were seeded at 4×10^5 cells/3.5-cm dish in Iscove's medium supplemented with 10% FCS but without Geneticin. At 24 h after transfection, the medium was removed, and the cells were UV irradiated (200 J/m^2) with Stratalinker UV cross-linker 1800. The treated cells were then cultured in fresh medium for 6 h. The cells were harvested, fixed with 4% paraformaldehyde, and stained with Hoechst 33342 (1 μg/ml) in serum-free medium for 10 min. After washing, the cell suspensions were dropped onto a slide. Green cells that also exhibited condensed chromatin were counted by means of the excitation from blue light (excited green fluorescent protein) and UV (excited Hoechst 33342). Apoptosis was expressed as the percentage of green cells with condensed chromatin.

Assay of DEVDase Activity. DEVDase activity was measured by using the Apo-ONE homogeneous caspase-3/7 assay kit (Promega, Tokyo, Japan) according to the manufacturer's instructions. The homogeneous caspase buffer and the caspase substrate Z-DEVD-R110 (rhodamine 110; bis-*N*-CBZ-L-aspartyl-L-glutamyl-L-valyl-L-aspartic acid amide) were mixed and added to each well of a 96-well plate that contained or did not contain samples (5×10^5 cells/well). The contents of the wells were gently mixed using a plate shaker at 300–500 rpm for 1 h at room temperature. Fluorescence of liberated R110 was measured at an excitation wavelength of 485 nm and an emission wavelength of 530 nm. DEVDase activity was expressed as an arbitrary unit.

RESULTS

Identification of API2-MALT1-Binding Proteins. The t(11;18) translocation, most commonly encountered in MALT lymphoma, was found to result in the fusion of an IAP, API2, and a novel protein, MALT1 (13–15). Although API2-MALT1 was shown to activate NF-κB activity through its homodimerization, it remains to be established whether this fusion protein can indeed exert an antiapoptotic function, which may be relevant to the pathogenesis of MALT lymphoma. As a first step in addressing this fundamental issue, we used a proteomic approach to identify API2-MALT1-binding proteins.

293T cells were transiently transfected with either an expression plasmid for NH_2-terminal FLAG-tagged API2-MALT1 or an empty plasmid. Cell lysates were prepared and incubated with anti-FLAG monoclonal antibody-coupled agarose beads. After extensive washing, associated proteins were eluted under acidic conditions from the beads and separated by SDS-PAGE. Five candidate protein bands were observed in a Coomassie Blue-stained gel (Fig. 1), but not in the control immunoprecipitate. These bands were excised from the gel and digested in gel with trypsin. The digested peptides were then analyzed directly by nanoscale high-performance liquid chromatography coupled to tandem mass spectrometry equipped with a nanoelectrospray ionization source. A database search of tandem mass spectra was performed with a Mascot Search Program.

Table 1 summarizes the peptides detected by mass spectrometry and their assigned proteins. Several peptides of HtrA2 and Smac were detected in bands D and E, respectively. The detection of HtrA2 and Smac as API2-MALT1-binding proteins is not surprising, in view of previous reports that these two proteins were identified as X-IAP-binding proteins (27, 28, 30, 32). HtrA2 is a mitochondrial serine protease and is released from mitochondria to the cytoplasm during apoptosis (30, 33–35). It also interacts with and cleaves IAPs, relieving caspase inhibition and promoting apoptosis (36, 37). Smac is also

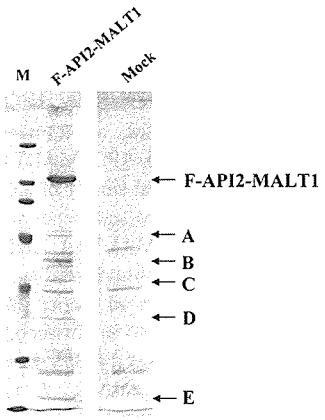

Fig. 1. Detection of apoptosis inhibitor 2 (API2)-MALT1-binding proteins. Overexpressed FLAG-tagged API2-MALT1 in 293T cells was affinity-purified using anti-FLAG M2 monoclonal antibody-coupled agarose beads. Eluted fractions were subjected to SDS-PAGE and stained with Coomassie Blue. Coeluted proteins with affinity-purified API2-MALT1 are represented by *A–E*.

normally a mitochondrial protein and, like HtrA2, is released to the cytoplasm concurrent with cytochrome *c* release during apoptosis (27, 28). It was found to interact with the baculovirus IAP repeat domain of IAPs. The binding of Smac to IAPs relieves the binding of IAPs to caspases, thus promoting caspase-mediated apoptosis. Several peptides of TRAF2 were detected in band 2. Because TRAF2 plays a crucial role in the tumor necrosis factor-stimulated apoptotic pathway, further study is warranted to examine the role of API2-MALT1 in this pathway. In addition to these regulators of apoptosis, three other proteins, Hsc70 (heat shock 70-kDa protein 8), GRP75 (stress-70 protein) and KIAA1892, were also detected in bands A and C. Identification of two members of the heat shock protein family of 70 kDa (HSP70) is intriguing because they not only function as molecular chaperones to facilitate protein folding and oligomerization, but also have been shown to exert antiapoptotic activity (38). KIAA1892 is a novel hypothetical protein whose function is currently unknown but is presumed to have WD-40 repeats. Given the fact that this novel protein has the potential to bind API2-MALT1, it will be interesting to further examine its function in the context of apoptosis as well as NF-κB signaling.

Unexpectedly, no peptides corresponding to BCL10 were detected that have been shown to form a complex with MALT1 through immunoglobulin-like domains (22, 23). To clarify this point, we performed Western blot analysis of API2-MALT1 immunoprecipitate samples (one-fourth of the proteins shown in Fig. 1) using BCL10 antibody. This analysis could not detect any apparent band corresponding to BCL10 (data not shown). One explanation for this nondetection would be that the amount of BCL10, if any, was undetectable in Coomassie Blue staining or below the detection limit of Western blot analysis. It is also conceivable that API2-MALT1 may have bypassed the normal BCL10 signaling pathway.

Interaction between API2-MALT1 and Smac. To verify the interaction between API2-MALT1 and Smac, expression plasmids for NH_2-terminal FLAG-tagged API2-MALT1 (F-API2-MAL1), COOH-terminal-deleted API2 (F-API2ΔC), NH_2-terminal-deleted MALT1 (F-MALT1ΔN), or an empty plasmid were transiently transfected together with an expression plasmid for Smac with a COOH-terminal myc tag (Smac-myc) into 293T cells. Transfected cell lysates were immunoprecipitated with anti-FLAG monoclonal antibody and then immunoblotted with anti-Myc monoclonal antibody. As shown in Fig. 2, the mature form of Smac-myc was coimmunoprecipitated with API2-MALT1 and API2ΔC. This indicates that API2-MALT1 indeed associates with exogeneously expressed Smac in the cells.

We next sought to examine whether API2-MALT1 interacts with endogenous Smac in cells. Expression plasmids for F-API2-MALT1, F-API2ΔC, F-MALT1ΔN, or an empty plasmid were transiently transfected into 293T cells. Transfected cell lysates were immunoprecipitated with anti-FLAG monoclonal antibody and then immunoblotted with anti-Smac monoclonal antibody. As shown in Fig. 3, endogeneous Smac was also immunoprecipitated with API2-MALT1, which strongly suggests that the interaction between API2-MALT1 and Smac could be physiologically significant. Interaction of API2-MALT1 with endogenous HtrA2 and TRAF2 was also confirmed by immunoprecipitation analysis (data not shown).

Table 1 *List of proteins identified as API2-MALT1-binding proteins*

Proteins	Bands	Peptides detected
HSC70 (HSP73)	Band A	VEIIANDQGNR
		NQVAMNPTNTVFDAK
		RFDDAVVQSDMK
		HWPFMVVNPAGRPK
		SFYPEEVSSMVLTK
		IINEPTAAAIAYGLDKK
GRP75 (75-kDa glucose-regulated protein, Stress-75 protein)		VQQTVQQDLFGR
TRAF2	Band B	VAMTAEACSR
		LDQDKIEALSSK
		DLAMADLEQK
		IYLNGDGTGR
Precursor HtrA2		YIGVMMLTLSPSILAELQLR
		AGLRPGDVILAIGEQMVQNAEDVYEAVR
KIAA1892	Band C	TLLATGGDNPNSLAIYR
HtrA2	Band D	AVPSPPPASPR
		SQYNFIADVVEK
		LLSGDTYEAVVTAVDPVADIATLR
		EPLPTLPLGR
		QGEFVVAMGSPFALQNTITSGIVSSAQRPAR
		VTAGISFAIPSDR
Smac	Band E	SEPHSLSSEALMR
		AVYTLTSLYR
		MNSEEEDEVMQVIIGAR
		LETTWMTAVGLSEMAAEAAYQTGADQASITAR
		LQVEEVHQLSR
		LAEAQIEELR
		AESEQEAYLRED

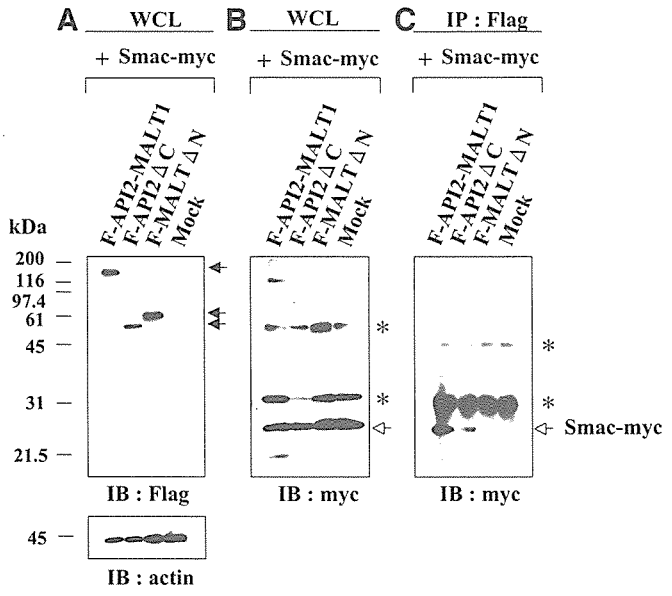

Fig. 2. Apoptosis inhibitor 2 (API2)-MALT1 binds to exogeneous Smac. FLAG-tagged API2-MALT1 plasmid, FLAG-tagged API2ΔC (amino acids 1–442), or FLAG-tagged MALT1ΔN [amino acids 217–813 (0.5 μg each)] was transfected with a COOH-terminal myc-tagged Smac plasmid (0.5 μg) into 293T cells, and whole cell lysates (*WCL*) were immunoprecipitated with anti-FLAG M2 monoclonal antibody. Whole cell lysates were analyzed with immunoblotting (*IB*) using anti-FLAG monoclonal antibody (*A*) or anti-Myc polyclonal antibody (*B*). Immunoprecipitates were analyzed with immunoblotting using anti-Myc polyclonal antibody (*C*). Nonspecific bands are shown by an *asterisk*.

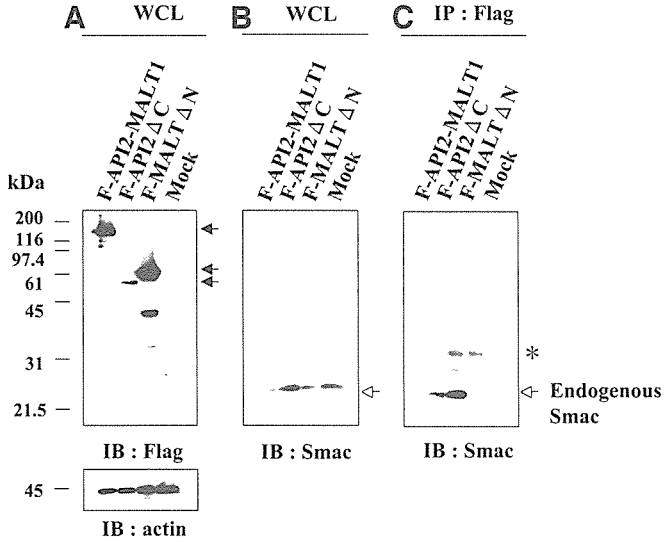

Fig. 3. Apoptosis inhibitor 2 (API2)-MALT1 binds to endogeneous Smac. Whole cell lysates (*WCL*) from the 293T cells transfected with a FLAG-tagged API2-MALT1 plasmid, FLAG-tagged API2ΔC (amino acids 1–442), or FLAG-tagged MALT1ΔN [amino acids 217–813 (0.5 μg each)] were immunoprecipitated with anti-FLAG M2 monoclonal antibody. Whole cell lysates were analyzed with immunoblotting (*IB*) using anti-FLAG monoclonal antibody (*A*) or anti-Smac polyclonal antibody (*B*). Immunoprecipitates were analyzed with immunoblotting using anti-Smac polyclonal antibody (*C*). Nonspecific bands are shown by an *asterisk*.

API2-MALT1 Confers Resistance to UV- and Etoposide-Induced Apoptosis. Because API2 is known to be an IAP (also known as c-IAP2), one can speculate that API2-MALT1 has a similar antiapoptotic function as well. Because no experimental evidence has been presented for such a function, however, we decided to test API2-MALT1 for this purpose. We chose a HeLa cell line in which several apoptotic stimuli including UV irradiation, chemotherapeutic agents, and tumor necrosis factor rapidly induce typical apoptotic changes characterized by chromatin condensation and DNA fragmentation. First, an API2-MALT1 expression plasmid was transiently transfected into HeLa cells, but the fusion protein was barely detectable by Western blot analysis of the whole cell lysates (data not shown). Therefore, we decided to establish stable transfectants expressing API2-MALT1. To this end, we transfected its linearized expression plasmid (PCXN2-FLAG-API2-MALT1) into HeLa cells, selected the cells with Geneticin, and finally cloned them by limiting dilution procedure. As a result, two independent clones expressing API2-MALT1, designated API2-MALT1-1 and API2-MALT1-2, were obtained and used for additional studies. As controls, two independent clones transfected with an empty plasmid only, designated Mock-1 and Mock-2, were also established.

It was noteworthy that when exposed to UV irradiation and treated with etoposide, both clones expressing API2-MALT1 (API2-MALT1-1 and API2-MALT1-2) showed significant attenuation, compared with that of the two control clones, in both UV- and etoposide-induced apoptosis as determined by the chromatin condensation (Figs. 4*A* and 5*A*). Thus, this provides for the first time direct evidence that API2-MALT1 can indeed confer resistance to apoptosis. We also measured DEVDase activity in these transfectants. Similarly, when exposed to UV irradiation or treated with etoposide, the two clones expressing API2-MALT1 showed significant attenuation of DEVDase activity (Figs. 4*B* and 5*B*), almost compatible with and further supporting the results of the apoptosis assay.

Because Smac has been shown to promote apoptosis in response to several stimuli such as UV irradiation that trigger the mitochondria-mediated apoptotic pathway, we examined the role of Smac in UV irradiation-induced apoptosis of the stable transfectants expressing API2-MALT1. To do so, we transiently transfected an expression plasmid for Smac-myc with a green fluorescent protein expression plasmid into the stable transfectants and then induced apoptosis by UV irradiation. Approximately 47–49% of Smac-transfected cells without expression of API2-MALT1 showed signs of apoptosis, as determined by the condensed chromatin. In contrast, only about 21–22% of Smac-transfected cells with stable expression of API2-MALT1 showed signs of apoptosis (Fig. 6). Thus, API2-MALT1 can confer significant resistance to apoptosis promoted by Smac in UV-irradiated HeLa cells.

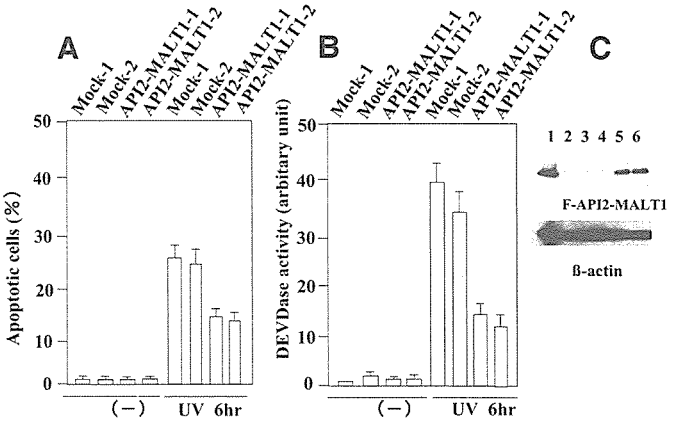

Fig. 4. Apoptosis inhibitor 2 (API2)-MALT1 confers resistance to apoptosis and suppresses DEVDase activity induced by UV irradiation. HeLa cells stably transfected with a FLAG-tagged API2-MALT1 plasmid (API2-MALT1-1 and API2-MALT1-2) or an empty plasmid (Mock-1 and Mock-2) were stimulated with UV irradiation (200 J/m^2). *A*, after 6 h, apoptosis was assessed by the presence of condensed chromatin. Data represent mean ± SD of triplicate samples. *B*, DEVDase activity (5 × 10^4 cells/sample) was also measured. *C*, whole cell lysates were analyzed with immunoblotting using anti-FLAG monoclonal antibody or anti-β-actin monoclonal antibody. *Lane 1*, 293T cells with API2-MALT1 expression (transient transfection); *Lane 2*, wild-type HeLa cells; *Lanes 3* and *4*, HeLa cells with empty vector (Mock-1 and Mock-2); *Lanes 5* and *6*, HeLa cells with API2-MALT1 stable expression (API2-MALT1-1 and API2-MALT1-2).

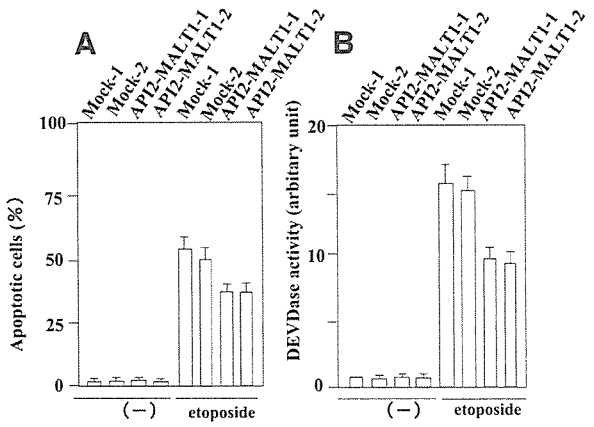

Fig. 5. Apoptosis inhibitor 2 (API2)-MALT1 confers resistance to apoptosis and suppresses DEVDase activity induced by etoposide treatment. HeLa cells stably transfected with a FLAG-tagged API2-MALT1 plasmid (API2-MALT1-1 and API2-MALT1-2) or an empty plasmid (Mock-1 and Mock-2) were treated with etoposide (100 μM) or DMSO for 12 h. *A*, apoptosis was assessed by the presence of condensed chromatin. *B*, DEVDase activity (5×10^4 cells/sample) was also measured. Data represent mean ± SD of triplicate samples.

DISCUSSION

Three distinct chromosomal translocations have been implicated in the pathogenesis of MALT lymphoma. The first, t(1;14), results in the juxtaposition of the *BCL10* gene to the immunoglobulin enhancer, in which BCL10 expression is thought to be deregulated (10, 11). The second, t(11;18), results in the synthesis of a novel fusion protein, known as API2-MALT1 (13–15). The more recently discovered third translocation, t(14;18), results in the juxtaposition of the *MALT1* gene to the immunoglobulin enhancer, in which deregulated MALT1 expression may occur (16, 17). We and others have recently shown (22, 23) that BCL10 and MALT1 form a specific complex within the cells and that these proteins synergize through homodimerization of MALT1 in activation of NF-κB. Furthermore, expression of API2-MALT1 was also shown to strongly activate NF-κB activity; however, ectopic expression of MALT1 alone, as can be expected to occur in MALT cases with t(14;18), was incapable of inducing NF-κB activity (22, 23). Thus, it remains to be established whether NF-κB activation by API2-MALT1 is indeed relevant to the pathogenesis of MALT lymphoma. Furthermore, no experimental evidence has been produced related to the fundamental question of whether API2-MALT1 can confer resistance to apoptosis.

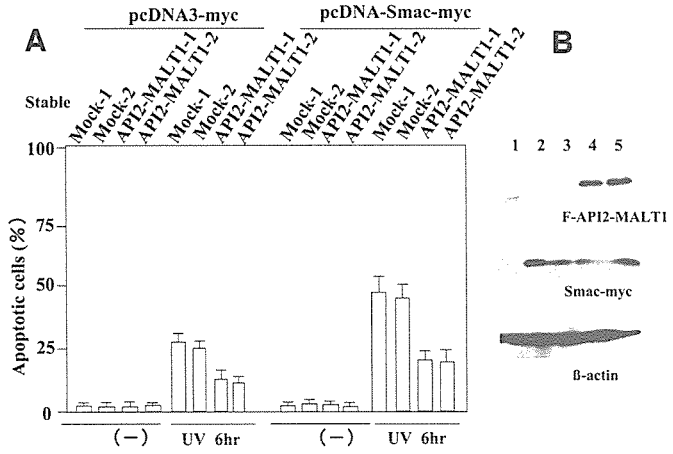

Fig. 6. Apoptosis inhibitor 2 (API2)-MALT1 confers resistance to apoptosis by action against the Smac-mediated apoptotic pathway. HeLa cells stably transfected with a FLAG-tagged API2-MALT1 plasmid (0.5 μg) or an empty plasmid (0.5 μg) were transiently transfected with a COOH-terminal myc-tagged Smac plasmid (2 μg) and a pEGFP plasmid (0.5 μg), incubated for 24 h, and then stimulated with UV irradiation (200 J/m^2). *A*, after 6 h, apoptosis was assessed by the presence of condensed chromatin and expressed as a percentage of apoptotic cells in total transfected green cells. Data represent mean ± SD from triplicate samples. *B*, whole cell lysates were analyzed with immunoblotting using anti-FLAG monoclonal antibody or anti-Myc polyclonal antibody or anti-β-actin monoclonal antibody. *Lane 1*, wild-type HeLa cells; *Lanes 2* and *3*, HeLa cells with empty vector; *Lanes 4* and *5*, HeLa cells with API2-MALT1 stable expression.

In the present study, we were able to identify API2-MALT1-binding proteins and to demonstrate for the first time that API2-MALT1 does exert an antiapoptotic effect against UV irradiation- and etoposide treatment-induced apoptosis in HeLa cells. This antiapoptotic effect may be mediated, at least in part, by action against the Smac-promoted apoptotic pathway. Because several apoptotic inhibitors have been shown to be up-regulated by NF-κB activation (39), our data do not entirely exclude the possibility that the antiapoptotic effect may be mediated, in part, by the secondary up-regulation of such apoptotic inhibitors. In a recent study, we examined whether API2-MALT1 has an antiapoptotic effect on murine interleukin 3-dependent hematopoietic Ba/F3 cells (27). For this purpose, stable transfectants expressing API2-MALT1 were established, and apoptosis was induced by interleukin 3 deprivation or UV irradiation. These results indicated that API2-MALT1 does not show obvious resistance to apoptosis induced by interleukin 3 deprivation or UV irradiation in Ba/F3 cells. Because NF-κB activation is generally thought to contribute to an antiapoptotic effect, we analyzed the nuclear NF-κB activity of these two cell lines by using the NF-κB ELISA kit (Oxford Biomedical Research, Inc.). However, this analysis revealed no significant difference in the amount of nuclear NF-κB between the two cell lines (data not shown), suggesting that the difference in antiapoptotic effect by API2-MALT1 may not be due to the difference in the cell lines' nuclear NF-κB activity. One reason for the difference between the results obtained for the HeLa and Ba/F3 cells would be that these two cell lines do not always use the same apoptotic signaling pathway.

We also examined the stability of ectopically expressed API2, MALT1, and API2-MALT1 by Western blot analysis of the cell lysates with or without treatment with MG132, a proteasome inhibitor (27). It was found that MALT1 is rapidly degraded via the ubiquitin-proteasome pathway, as is the case with API2. On the synthesis of fusion, API2-MALT1 was readily detectable even without MG132, suggesting that this fusion protein becomes stable against the ubiquitin-proteasome pathway (27). Thus, increased stability of API2-MALT1 would be expected to augment counteraction against or synergy with the functions of its binding partners including Smac, HtrA2, and TRAF2.

To the best of our knowledge, this is the first report demonstrating that API2-MALT1 acts as an antiapoptotic regulator, which may be mediated, at least in part, by neutralizing apoptosis promoted by Smac. It stands to reason that Smac would not be the only target for the antiapoptotic effect exerted by API2-MALT1, and indeed, we have identified TRAF2, HtrA2, KIAA1892, and HSP70s as other potential API2-MALT1-binding proteins. Given that Smac, TRAF2, and HtrA2 function as *bona fide* regulators of apoptosis, it is tempting to speculate that the KIAA1892 protein and two Hsp70s exert the same effect. Because recent studies of the *BCL10* and *MALT1* knockout mice provide evidence that both BCL10 and MALT1 participate in linking antigen receptor signaling and NF-κB activation (29–31) and exogeneously expressed API2-MALT1 was shown to enforce activation of NF-κB activity (27, 28), it will be of particular importance to pursue the possible roles of API2-MALT1-binding proteins in antigen receptor signaling. It is hoped that additional studies will provide further insight into the biological functions of API2-MALT1 and ultimately lead to new diagnostic and therapeutic advances for dealing with MALT lymphoma, a human lymphoma that has been attracting special attention.

REFERENCES

1. Isaacson P, Wright DH. Malignant lymphoma of mucosa-associated lymphoid tissue. A distinctive type of B-cell lymphoma. Cancer (Phila) 1983;52:1410–6.
2. Harris NL, Jaffe ES, Stein H, et al. A revised European-American classification of lymphoid neoplasms: a proposal from the International Lymphoma Study Group. Blood 1994;84:1361–92.
3. Isaacson PG, Muller-Hermelink HK, Piris MA, et al. Extranodal marginal zone B-cell lymphoma of mucosa-associated lymphoid tissue (MALT lymphoma). In: Jaffe ES, Harris NL, Stein H, Vardiman JW, editors. WHO Classification of Tumours: Pathology and Genetics. Tumours of Haemopoietic and Lymphoid Tissues. Lyon, France: IARC Press; 2001. p. 121–6.
4. The Non-Hodgkin's Lymphoma Classification Project. A clinical evaluation of the International Lymphoma Study Group Classification of Non-Hodgkin's Lymphoma. Blood 1997;89:3909–18.
5. Horseman D, Gascoyne R, Klasa R, Coupland R. t(11;18)(q21;q21): a recurring translocation in lymphomas of mucosa-associated lymphoid tissue (MALT)? Genes Chromosomes Cancer 1992;4:183–7.
6. Wotherspoon AC, Pan L, Diss TC, Isaacson PG. Cytogenetic study of B-cell lymphoma of mucosa-associated lymphoid tissue. Cancer Genet Cytogenet 1992;58: 35–8.
7. Wotherspoon AC, Finn TM, Isaacson PG. Trisomy 3 in low-grade B-cell lymphomas of mucosa-associated lymphoid tissue. Blood 1995;85:2000–4.
8. Dierlamm J, Pittaluga S, Wlodarska I, et al. Marginal zone B-cell lymphomas of different sites share similar cytogenetic and morphologic features. Blood 1996;87: 299–307.
9. Auer IA, Gascoyne RD, Connors JM, et al. t(11;18)(q21;q21) is the most common translocation in MALT lymphomas. Ann Oncol 1997;8:979–85.
10. Willis TG, Jadayel DM, Du M-Q, et al. Bcl10 is involved in t(1;14)(p22;q32) of MALT B-cell lymphoma and mutated in multiple tumor types. Cell 1999;96:35–45.
11. Zhang Q, Siebert R, Yan M, et al. Inactivating mutations and overexpression of BCL10, a caspase recruitment domain-containing gene, in MALT lymphoma with t(1;14)(p22;q32). Nat Genet 1999;22:63–8.
12. Ott G, Katzenberger T, Greiner A, et al. The t(11;18)(q21;q21) chromosome translocation is a frequent and specific aberration in low-grade but not high-grade malignant non-Hodgkin's lymphomas of the mucosa-associated lymphoid tissue (MALT-) type. Cancer Res 1997;57:3944–8.
13. Akagi T, Motegi M, Tamura A, et al. A novel gene, MALT1 at 18q21, is involved in t(11;18)(q21;q21) found in low-grade B-cell lymphoma of mucosa-associated lymphoid tissue. Oncogene 1999;18:5785–94.
14. Dierlamm J, Baens M, Wlodarska I, et al. The apoptosis inhibitor gene API2 and a novel 18q gene, MLT, are recurrently rearranged in the t(11;18)(q21;q21) associated with mucosa-associated lymphoid tissue lymphomas. Blood 1999;93:3601–9.
15. Morgan JA, Yin Y, Borowsky AD, et al. Breakpoints of the t(11;18)(q21;q21) in mucosa-associated lymphoid tissue (MALT) lymphoma lie within or near the previously undescribed gene MALT1 in chromosome 18. Cancer Res 1999;59:6205–13.
16. Sanchez-Izquierdo D, Buchonnet G, Siebert R, et al. MALT1 is deregulated by both chromosomal translocation and amplification in B-cell non-Hodgkin lymphoma. Blood 2003;101:4539–46.
17. Streubel B, Lamprecht A, Dierlamm J, et al. t(14;18)(q32;q21) involving IGH and MALT1 is a frequent chromosomal aberration in MALT lymphoma. Blood 2003; 101:2335–9.
18. Murga Penas EM, Hinz K, Roser K, et al. Translocations t(11;18)(q21;q21) and t(14;18)(q32;q21) are the main chromosomal abnormalities involving MLT/MALT1 in MALT lymphomas. Leukemia (Baltimore) 2003;17:2225–59.
19. Remstein ED, Kurtin PJ, Einerson RR, Paternoster SF, Dewald GW. Primary pulmonary MALT lymphomas show frequent and heterogeneous cytogenetic abnormalities, including aneuploidy and translocations involving API2 and MALT1 and IGH and MALT1. Leukemia (Baltimore) 2004;18:156–60.
20. Rothe M, Pan MG, Henzel WJ, Ayres TM, Goeddel DV. The TNFR2-TRAF signaling complex contains two novel proteins related to baculoviral inhibitor of apoptosis proteins. Cell 1995;83:1243–52.
21. Hofmann K, Bucher P, Tschopp J. The CARD domain: a new apoptotic signalling motif. Trends Biochem Sci 1997;22:155–6.
22. Uren AG, O'Rourke K, Aravind L, et al. Identification of paracaspases and metacaspases, two ancient families of caspase-like proteins, one of Which plays a key role in MALT lymphoma. Mol Cell 2000;6:961–7.
23. Lucas PC, Yonezumi M, Inohara N, et al. Bcl10 and MALT1, independent targets of chromosomal translocation in malt lymphoma, cooperate in a novel NF-κB signaling pathway. J Biol Chem 2001;276:19012–9.
24. Ruland J, Duncan GS, Elia A, et al. Bcl10 is a positive regulator of antigen receptor-induced activation of NF-κB and neural tube closure. Cell 2001;104:33–42.
25. Ruland J, Duncan GS, Wakeham A, Mak TW. Differential requirement for malt1 in T and B cell antigen receptor signaling. Immunity 2003;19:749–58.
26. Ruefli-Brasse AA, French DM, Dixit VM. Regulation of NF-κB-dependent lymphocyte activation and development by paracaspase. Science (Wash DC) 2003;302: 1581–4.
27. Du C, Fang M, Li Y, Li L, Wang X. Smac, a mitochondrial protein that promotes cytochrome c-dependent caspase activation by eliminating IAP inhibition. Cell 2000; 102:33–42.
28. Verhagen AM, Ekert PG, Pakusch M, et al. Identification of DIABLO, a mammalian protein that promotes apoptosis by binding to and antagonizing IAP proteins. Cell 2000;102:43–53.
29. Izumiyama K, Nakagawa M, Yonezumi M, et al. Stability and subcellular localization of API2-MALT1 chimeric protein involved in t(11;18)(q21;q21) MALT lymphoma. Oncogene 2003;22:8085–92.
30. Suzuki Y, Imai Y, Nakayama H, et al. Serine protease, HtrA2, is released from the mitochondria and interacts with XIAP, inducing cell death. Mol Cell 2001;8:613–21.
31. Shevchenko A, Wilm M, Vorm O, Mann M. Mass spectrometric sequencing of proteins silver-stained polyacrylamide gels. Anal Chem 1996;68:850–8.
32. Vaux DL, Silke J. Mammalian mitochondrial IAP binding proteins Biochem Biophys Res Commun 2003;304:499–504.
33. Hegde R, Srinivasula SM, Zhang Z, et al. Identification of Omi/HtrA2 as a mitochondrial apoptotic serine protease that disrupts inhibitor of apoptosis protein-caspase interaction. J Biol Chem 2002;277:432–8.
34. Martins LM, Iaccarino I, Tenev T, et al. The serine protease Omi/HtrA2 regulates apoptosis by binding XIAP through a reaper-like motif. J Biol Chem 2002;277:439–44.
35. Verhagen AM, Silke J, Ekert PG, et al. HtrA2 promotes cell death through its serine protease activity and its ability to antagonize inhibitor of apoptosis proteins. J Biol Chem 2002;277:445–54.
36. Srinivasula SM, Gupta S, Datta P, et al. Inhibitor of apoptosis proteins are substrates for the mitochondrial serine protease Omi/HtrA2. J Biol Chem 2003;278:31469–72.
37. Yang Y, Fang S, Jensen JP, Weissman AM, Ashwell JD. Ubiquitin protein ligase activity of IAPs and their degradation in proteasomes in response to apoptotic stimuli. Science (Wash DC) 2000;288:874–7.
38. Parcellier A, Gurbuxani S, Schmitt E, Solary E, Garrido C. Heat shock proteins, cellular chaperones that modulate mitochondrial cell death pathways. Biochem Biophys Res Commun 2003;304:505–12.
39. Mayo MW, Baldwin AS. The transcription factor NF-κB: control of oncogenesis and cancer therapy resistance. Biochim Biophys Acta 2000;1470:M55–62.

THE JOURNAL OF BIOLOGICAL CHEMISTRY
Vol. 279, No. 30, Issue of July 23, pp. 30983–30993, 2004
Printed in U.S.A.

Differentiation-dependent Sensitivity to Apoptogenic Factors in PC12 Cells*

Received for publication, January 21, 2004, and in revised form, May 7, 2004
Published, JBC Papers in Press, May 7, 2004, DOI 10.1074/jbc.M400692200

Sheela Vyas‡§, Philippe Juin¶, David Hancock‖, Yasuyuki Suzuki, Ryosuke Takahashi**, Antoine Triller‡, and Gerard Evan‡‡**

*From the ‡INSERM U497, Ecole Normale Supérieure, 46, rue d'Ulm, Paris 75005, ¶INSERM U419, 9 Quai Moncousu, 44035 Nantes Cedex, France, the ‖Signal Transduction Laboratory, Cancer Research UK, 44 Lincoln's Inn Fields, London WC2A 3PX, United Kingdom, the **Laboratory for Motor System Neurodegeneration, RIKEN Brain Science Institute, Saitama, 351-0198, Japan, and the ‡‡University of California at San Francisco Cancer Center, San Francisco, California 94143-0875*

We have investigated the role of the mitochondrial pathway during cell death following serum and nerve growth factor (NGF)/dibutyryl cyclic AMP (Bt_2cAMP) withdrawal in undifferentiated or NGF/Bt_2cAMP-differentiated PC12 cells, respectively. Holocytochrome *c*, Smac/DIABLO, and Omi/HtrA2 are released rapidly following trophic factor deprivation in PC12 cells. Bcl-2 and Akt inhibited this release. The protection, however, persisted longer in differentiated PC12 cells. In differentiated, but not undifferentiated cells, Bcl-2 and Akt also inhibited apoptosis downstream of holocytochrome c release. Thus, undifferentiated PC12 cells showed marked sensitivity to induction of apoptosis by microinjected cytochrome *c* even in the presence of NGF, Bcl-2, or Akt. In contrast, in differentiated cells these factors suppressed cell death. Consistent with these observations, *in vitro* processing of procaspase 9 in response to cytochrome *c* was observed in extracts from undifferentiated but not differentiated cells expressing Akt or Bcl-2. Endogenous caspase 9 was cleaved during cell death, whereas dominant negative caspase 9 inhibited cell death. The results from determining the role of inhibitors of apoptosis (IAPs) suggest that acquisition of inhibition by IAPs is part of the differentiation program. Ubiquitin-ΔN-AVPI Smac/DIABLO induced cell death in differentiated cells only. c-IAP-2 is unregulated in differentiated cells, whereas X-linked IAP levels decreased in these cells coincident with cell death. Moreover, expressing X-linked IAP rendered undifferentiated cells resistant to microinjected cytochrome *c*. Overall, the inhibitory regulation, of cell death at the level of release of mitochondrial apoptogenic factors and at post-mitochondrial activation of caspase 9 observed in differentiated PC12 cells, is reduced or absent in the undifferentiated counterparts.

Cell death is essential for the development of the nervous system, where neurogenic precursor cells are produced in excess and then eliminated at specified times during the migration and differentiation of distinct populations of neurons (1–3). Conversely, suppression of the cell death is vital for the maintenance of non-dividing neurons after terminal differentiation.

Compelling experimental evidence that apoptosis is critical for nervous system development has emerged from *in vivo* studies in mice carrying null mutations for various components of the apoptotic machinery such as *Bcl-x_L*, *caspases 3* and *9*, and *Apaf-1* genes (4–7). In all such cases, gross organizational anomalies in developing CNS contribute to the observed prenatal lethality. Thus, in the absence of *Bcl-X_L*, excessive death of differentiating neuronal cells occurs in brainstem and spinal cord. Embryonic mice with null mutations in *Apaf-1*, *caspase 3*, or *caspase 9* display morphological CNS abnormalities, as a result of supernumerary cells expanded ventricular zone and forebrain protrusions occur. The general inference from detailed analyses in such mice, as well as in the double knock-out mutant mice such as *Bcl-$x_L^{-/-}$/caspase $3^{-/-}$* and *Bcl-$x_L^{-/-}$/caspase $9^{-/-}$*, is that cell death in CNS development not only serves to match the size of a neuronal population to its target field but is also vital for global morphogenesis of the nervous system. Additionally, such observations suggest that the mechanisms responsible for early cell death in neural progenitor cells may differ from those in post-mitotic neurons. In neural progenitor cells, caspase 3 or 9 function is independent of Bcl-x_L regulation, whereas in post-mitotic neurons, Bcl-x_L acts upstream of caspases 9 and 3 in an epistatic manner (8–10). Apoptotic pathways are also activated during inappropriate neuronal death that occurs in acute and chronic neurodegenerative diseases. For example, activated forms of caspases are observed in degenerating neurons following stroke and in Parkinson or Alzheimer diseases (11, 12).

Because caspases are the final implementers of apoptosis, tight control of caspase activation is crucial for long term survival of post-mitotic neurons. Caspases are synthesized as inactive zymogens that are catalytically activated by specific proteolytic cleavage, either by the action of upstream caspases or, in the case of the apical caspases, through autoactivation following their assembly into multimeric protein complexes (13–15). Mitochondria play a key role in orchestrating activation of one key apical caspase, caspase 9. In response to many mechanistically diverse pro-apoptotic triggers, mitochondria release multiple pro-apoptotic effectors from their inter-membrane space. One of these is holocytochrome *c* (hcC),[1] which, once in the cytosol, forms a complex with and activates the Apaf-1-caspase-9 holoenzyme to generate an active "apopto-

* This work was supported by an INSERM/Medical Research Council travel fellowship (to S. V.) and by the Association Francaise contre les Myopathies and Institut pour la Recherche sur la Moelle Epinière. The costs of publication of this article were defrayed in part by the payment of page charges. This article must therefore be hereby marked "*advertisement*" in accordance with 18 U.S.C. Section 1734 solely to indicate this fact.

§ To whom correspondence should be addressed. Tel.: 33-1-44-32-35-33; Fax: 33-1-44-32-36-54; E-mail: vyas@wotan.ens.fr.

[1] The abbreviations used are: hcC, holocytochrome *c*; NGF, nerve growth factor; Bt_2cAMP, dibutyryl cyclic AMP; PBS, phosphate-buffered saline; GFP, green fluorescent protein; Ub, ubiquitin; IAP, inhibitor of apoptosis; XIAP, X-linked IAP; Smac, second mitochondrial derived activator of caspases.

some" (16). Upon receipt of an apoptotic signal, mitochondria synchronously release all of their cytochrome *c* (17), although the exact molecular mechanism of its translocation remains unresolved (18–20). Several other apoptogenic factors are also released from mitochondria during cell death, among them Smac/DIABLO and Omi/HtrA2, which both act by binding to and inhibiting IAP function, releasing the activities of caspases 9, 3, and 7 (21–23). Substantial experimental evidence indicates that pro-apoptotic Bcl-2 family members such as Bax, Bak, and Bad promote hcC release and, therefore, trigger cell death, whereas the anti-apoptotic members Bcl-2 and Bcl-x_L prevent cell death by inhibiting hcC release. In addition, exogenous survival factors such as NGF and insulin-like growth factor-1 inhibit cytochrome *c* release, in part through an Akt-dependent phosphorylation and deactivation of Bad (24, 25).

Non-differentiated, proliferating PC12 (pheochromocytoma) cells undergo cell death upon withdrawal of serum. However, they can be rescued by acute treatment with various survival factors such as insulin-like growth factor-1 or NGF or by administration of Bt_2cAMP (26, 27). In addition to signaling survival, some of these factors also induce differentiation of PC12 cells, although any mechanistic relationship between survival and differentiation is unclear. Although caspase-mediated cell death following withdrawal of serum or NGF in PC12 cells and in primary sympathetic neurons has been well studied (28–30), whether differentiation has a role in regulation of caspases has not been analyzed.

We have previously shown that NGF/Bt_2cAMP-induced differentiation leads to these cells becoming terminally and irreversibly differentiated, and, upon withdrawal of NGF and Bt_2cAMP, they die asynchronously by apoptosis (26). In this study, we have investigated the role of cytochrome *c*/caspase 9 activation during cell death induced by trophic factor withdrawal in undifferentiated and NGF/Bt_2cAMP-differentiated PC12 cells. In addition, the regulation of this cell death pathway by the pro-survival effectors Akt and Bcl-2 was examined.

EXPERIMENTAL PROCEDURES

Cell Culture and Preparation of Stably Expressing Cell Lines—Undifferentiated PC12 cells were cultivated in RPMI 1640 medium containing 10% fetal calf serum and 5% horse serum. They were induced to differentiate in modified L15 medium containing 5% fetal calf serum, 10% horse serum, and 50 ng/ml NGF (7S form, Roche Applied Science) as previously described (26). After 3 days, 200 μM Bt_2cAMP (Sigma) was added, and the cells were differentiated for a further 4–5 days. Cell death was induced in undifferentiated cells (50–60% confluent) by serum withdrawal for 24–48 h. In differentiated cells, apoptosis was triggered by removal of NGF/Bt_2cAMP from the medium.

Hbcl-2 (human *bcl-2*) cDNA inserted in pRc/CMV expression vector was electroporated into PC12 cells, G418-resistant hBcl-2 clones were selected, and expression of hBcl-2 protein was verified by Western blot analysis. DNA comprising v-*Akt-gag* inserted into the pLXSN vector was transfected into the GP+E packaging cell line, and ecotropic virus-containing supernatant was harvested and filtered. PC12 cells were treated for 5 h with this virus supernatant containing 8 μg/ml Polybrene. The virus supernatant was then replaced with RPMI/serum medium, and 24 h later the cells were selected in G418 (250 μg/ml) for a further 3 weeks, after which individual colonies were used for further analyses. cDNA encoding the dominant negative caspase 9 C287S point mutant fused to the FLAG epitope (C9DN) (31) was inserted into pcDNA3.1 vector and transfected into PC12 cells by LipofectAMINE treatment, and the G418-resistant pools of clones were selected. Expression of C9DN was verified by immunoblot analysis. G418-resistant PC12 cells in the presence of doxycycline (Sigma, 0.5 μg/ml) transfected with cDNA encoding for mouse XIAP in pN-21 tetracycline-repressible vector, were selected for XIAP function in undifferentiated cells. Parallel cultures of cells were transfected with empty plasmid vector and used as controls (PC12/C).

Microinjection—Undifferentiated and differentiated PC12 cells were cultivated on glass-bottomed coverslip dishes (MatTek Corp.). Cytochrome *c* (Sigma) solution was freshly prepared at desired concentrations and then mixed thoroughly with 0.4% (final concentration) rhodamine-dextran (Sigma), a fluorescent marker. In differentiated cells, where appropriate NGF/Bt_2cAMP was withdrawn just prior to microinjections. Doxycycline was withdrawn ~16 h prior to microinjections of XIAP/PC12 cells. After microinjections, the medium was replaced and cell death monitored at timed intervals. Microinjection parameters were kept constant: an automated Eppendorf microinjection system was used in which the pressure was held at 120 heptopascals and time at 0.2 s. Approximately 200–350 cells were microinjected for each study, and culture medium was replaced immediately after microinjections. Viability of microinjected cells was monitored by direct fluorescent microscopy at various time points. At high (×63 or ×100) magnification, rhodamine fluorescence was easily detectable in the cytoplasm and neurites of differentiated cells but excluded from the nuclei. The characteristic morphology of apoptosis, rounding up of cells accompanied by homogenous distribution of the rhodamine marker and fragmentation of nuclei and/or cytoplasm into apoptotic bodies, allowed us to quantify the apoptotic *versus* viable cells.

Transient Transfections—Undifferentiated and differentiated PC12 cells, cultured in 4-well multidishes, were transfected with 0.2 μg of pEGFP plus 0.8 μg of Ub-ΔN-AVPI-Myc or Ub-ΔN-MVPI Smac/DIABLO-Myc cloned in pcDNA3, using LipofectAMINE 2000 (Invitrogen) according to the manufacturer's instructions. Medium containing LipofectAMINE 2000 was removed after 6 h and replaced with appropriate normal medium. 24 h post-transfection, the cells were deprived of trophic support for 8 or 24 h and after PBS wash, were fixed with 4% paraformaldehyde. The cells were treated with 1 μg/ml Hoescht, and cell death was quantified by counting apoptotic nuclei of GFP-positive cells. It was verified that GFP-positive cells also express Ub-ΔN-AVPI-Myc or Ub-ΔN-MVPI Smac/DIABLO-myc by immunofluorescence using 9E10 anti-myc antibody.

Biochemical Methods—Soluble cytoplasmic and membrane fractions were prepared as described previously (32). Briefly, both undifferentiated and differentiated PC12 cells were cultured in 15-cm culture dishes. Cells in culture dishes were rinsed twice using ice-cold phosphate-buffered saline (PBS). They were harvested by adding a small volume (100 μl) of cold sucrose-supplemented cell extract buffer (300 mM sucrose, 10 mM HEPES (pH 7.4), 5 mM $MgCl_2$, 5 mM EGTA, 1 mM dithiothreitol, 10 mM cytochalasin B, and 1 mM phenylmethylsulfonyl fluoride) to culture dishes, scraped, and pelleted. The pellets were resuspended in the above buffer, incubated on ice for 30 min, homogenized, and centrifuged at 14,000 × *g* for 15 min. The supernatants comprising the cytoplasmic/soluble fraction and pellets (heavy membrane fraction) were separated and stored at −80 °C. Total cell lysates were prepared, after PBS wash, by directly adding Laemmli buffer containing protease inhibitors to cells; the samples were boiled and centrifuged. Total protein was quantified by the method of Bradford. The antibodies used were cytochrome *c* (antibody at 1:1000 dilution; BD Pharmingen, clone 7H8.2C12), cytochrome oxidase IV (antibody at 1:1000 dilution, Molecular Probes), Smac/DIABLO (produced at ICR, antibody at 1:1500 dilution), Omi/HtrA2 (antibody at 1:1000 dilution (22)), caspase 9 (antibody at 1:1000 dilution, Stressgen), c-IAP-2 (antibody at 1:1000 dilution, Santa Cruz Biotechnology), and XIAP (antibody at 1:1000 dilution (22)). The Smac/DIABLO antibody was made against mature N-terminal region (Cancer Research, UK), and the specificity was verified by peptide block. For immunoblot assays, 14, 12, or 10% SDS-PAGE gels were loaded with lysates containing appropriate concentrations of total protein. After transfer to Immobilon P membrane and incubation with primary and secondary antibodies, the signals were developed using enhanced chemiluminescence kit (Amersham Biosciences).

In Vitro Procaspase 9 Processing—Procaspase 9 cDNA in pBluescript was *in vitro* transcribed with T3 RNA polymerase, translated, and radiolabeled with ^{35}S-labeled methionine/cysteine (Amersham Biosciences) using the TnT-coupled transcription/translation rabbit reticulocyte lysate system (Promega). Processing of *in vitro*-translated procaspase 9 product by the cytoplasmic extracts prepared from PC12 cells was assayed essentially as described previously (31). Briefly, 1.5 μl of [^{35}S]procaspase 9 product was incubated at 30 °C for 30 min with cytoplasmic extracts containing 20 μg of protein (prepared as described above for hcC analysis) in the presence or absence of cytochrome *c* (10 mM) and dATP (1 mM): all in 10-ml total volume. Laemmli buffer was added, and the samples were boiled and fractionated by SDS-PAGE analysis followed by autoradiography.

RESULTS

Cytochrome c Release in Undifferentiated PC12 Cells following Withdrawal of Serum—The kinetics of subcellular redistri-

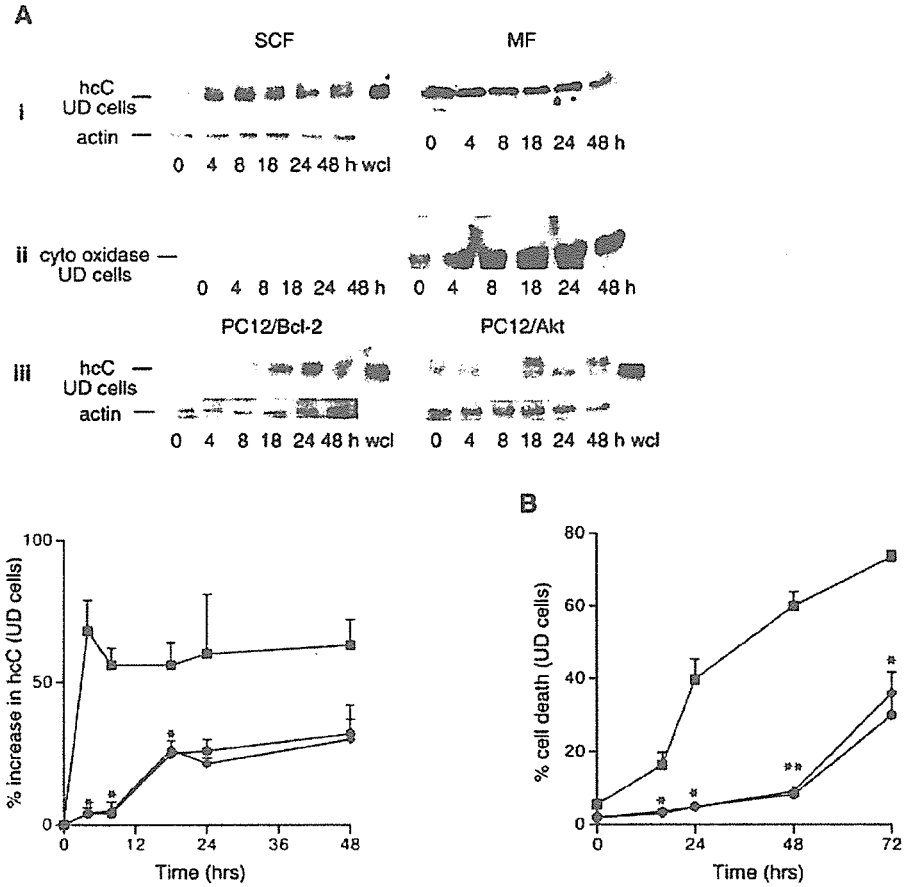

FIG. 1. **Kinetics of holocytochrome *c* (hcC) release and cell death in undifferentiated (*UD*) PC12 control (*PC12/C*), PC12/Bcl-2, and PC12/Akt cells.** *A*, soluble cytosolic fraction (*SCF*) and membrane fractions (*MF*) were prepared from serum containing 0, 4, 8, 18, 24, 36, and 48-h serum-deprived cells. An aliquot (whole cell lysate, *wcl*) was taken from serum-containing cells before fractionation and solubilized by adding 0.1% Triton X-100. 20 μg of total protein of SF and whole cell lysate (*wcl*) and 10 μg of MF was used for analysis of cytochrome *c* content. The autoradiograms of a representative experiment are shown. *i*, hcC in SCF and MF of PC12/C cells; *ii*, hcC immunoblot was stripped and reprobed with anti-cytochrome oxidase IV antibody; the protein is present only in MF; *iii*, hcC in SCF and wcl of PC12/Bcl-2 and PC12/Akt cells deprived of serum up to 48 h. The SCF blots were reprobed with actin as control for protein loading. The autoradiogram signals of SCF blots were densitometrically quantified (*bottom left panel*) using Gel Analyst software program. These results, which represent data from 3–5 experiments for each cell type: PC12/C (*solid square*), PC12/Bcl-2 (*solid diamond*), and PC12/Akt (*solid circle*), are expressed as % increase in hcC, mean ± S.E. using the 0 h value as control. *, p value < 0.05, PC12/Bcl-2 or Akt *versus* PC12/C (Student's t test, two-tailed). *B*, undifferentiated PC12/C (*solid square*), PC12/Bcl-2 (*solid diamond*), and PC12/Akt (*solid circle*) cells were deprived of serum for 18, 24, 48, and 72 h, fixed with 4% paraformaldehyde, and nuclei were stained with 1 μg/ml Hoechst 33258. Apoptotic nuclei were quantified by analyzing five random fields, each field comprising ~150 nuclei. Each time point was assayed in quadruplicate; the results are expressed as % mean ± S.E. of at least three experiments. p values: *, <0.05 and **, 0.01; PC12/Bcl-2 and Akt *versus* PC/12 cells (Student's t test, two-tailed).

bution of hcC from mitochondria to cytosol in PC12 cells following withdrawal of trophic support was first analyzed. The amount of hcC in the membrane fraction containing intact mitochondria (verified by electron microscopy) *versus* the soluble cytoplasmic fraction was determined by immunoblotting. Proliferating undifferentiated PC12 cells maintained in high serum exhibited negligible cytoplasmic hcC. However, withdrawal of serum resulted in a rapid increase in cytosolic hcC, evident by 4 h and persisting at all the time points tested (Fig. 1*A*, *panel i*). In contrast to hcC, the integral mitochondrial protein, cytochrome oxidase IV was retained within the membrane fraction (Fig. 1*A*, *panel ii*). The cytosolic accumulation of hcC precedes cell death that begins around 18 h after serum deprivation (Fig. 1*B*).

Because Akt and Bcl-2 can suppress the release of hcC from mitochondria and inhibit apoptosis in several cell types (25, 33), we next assayed cytochrome *c* translocation following serum deprivation in PC12 cells constitutively expressing either active v-*Akt-gag* (PC12/Akt) or h*Bcl-2* (PC12/Bcl-2). Each study was conducted in two independent clones in which expression of either v-Akt-gag or hBcl-2 had been previously verified by immunoblotting (data not shown). In addition, the activated status of v-Akt-gag was confirmed with an antibody specific for phosphorylated Akt at Ser-473 (data not shown). The PC12/Akt and PC12/Bcl-2 clones used each expressed comparable levels of v-*Akt-gag* or h*Bcl-2*, respectively. During the 24- to 48-h time period of serum deprivation, expression of either v-*Akt-gag* or h*Bcl-2* significantly inhibited cell death in undifferentiated PC12 cells (Fig. 1*B*). For example, upon withdrawal of serum for 24 h, we observed 40 ± 5.5% cell death in control cells compared with <5% in either Akt- or Bcl-2-expressing clones. However, such protection was not absolute, because more extended 72-h serum deprivation elicited some 30% death in both PC12/Bcl-2 and PC12/Akt cells (compared with 80% in PC12 control cells) (Fig. 1*B*). Immunoblot analysis of hcC levels in serum-deprived PC12/Akt and PC12/Bcl-2 cells showed that cytoplasmic hcC levels only rise ~18 h after withdrawal of serum (Fig. 1*A*, *panel iii*). The quantification of signals revealed that the accumulation of hcC in cytoplasm of these cells was less than in control PC12 cells. Analysis of hcC in whole cell lysates showed comparable levels of hcC in PC12/control, PC12/Bcl-2, and PC12/Akt cells. Thus both Bcl-2 and Akt act to

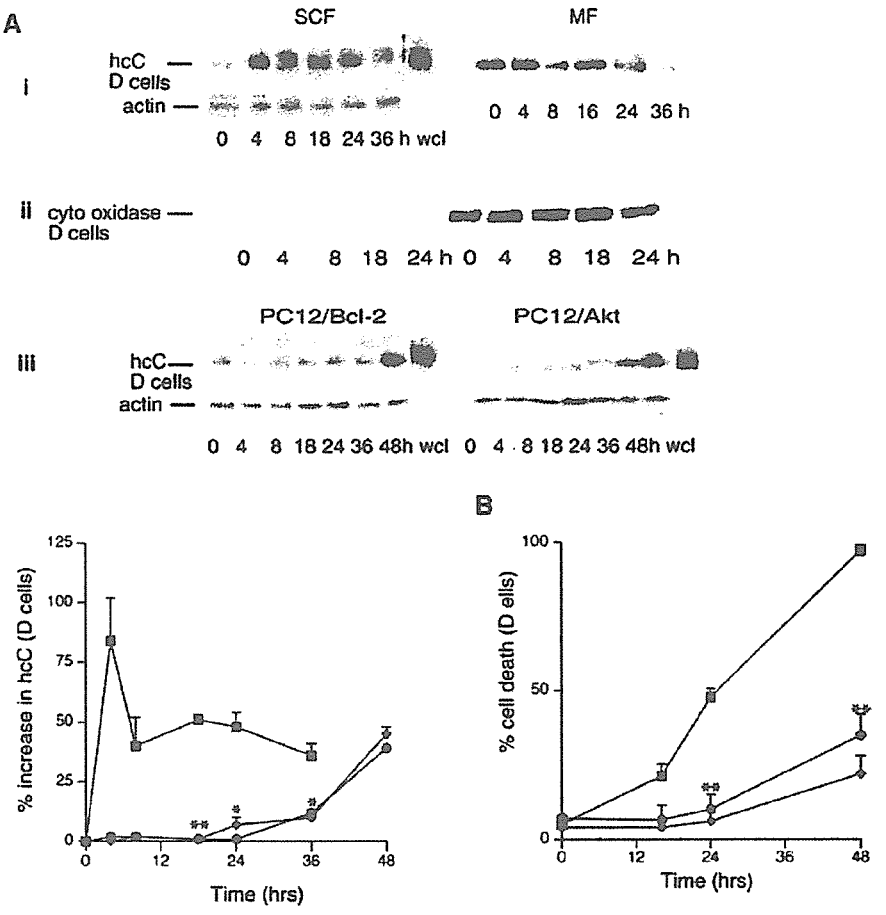

FIG. 2. **Holocytochrome c (hcC) release and cell death after withdrawal of NGF/Bt_2cAMP from NGF/Bt_2cAMP differentiated (*D*) PC12/C, PC12/Bcl-2, and PC12/Akt cells.** PC12 cells were differentiated with NGF/Bt_2cAMP followed by withdrawal of the latter at different times (h) as indicated. *A*, hcC content was analyzed in soluble cytosolic fraction (*SCF*) and membrane fraction (*MF*) at different times following NGF/Bt_2cAMP withdrawal. 20 μg of total protein of SCF and whole cell lysate (*wcl*) and 10 μg of MF were used for immunoblot assays. Results of a representative experiment of hcC content are shown in the *left panel*: *i*, hcC protein content in SCF, wcl, and MF of differentiated PC12/C cells (0) deprived of NGF/Bt_2cAMP for up to 36 h; *ii*, hcC immunoblot was stripped and reprobed for cytochrome *c* oxidase IV, which was present only in the MF; *iii*, hcC content in SCF of differentiated PC12/Bcl-2 and PC12/Akt cells (0 h) deprived of NGF/Bt_2cAMP for up to 48 h. Results of actin as control for protein loading are shown at the *bottom*. hcC in SCF was quantified (*bottom left panel*), the results are expressed as % increase in hcC, mean ± S.E. using 0 h value as control (n = 4). p values: *, <0.05; **, 0.01; PC12/Bcl-2 or Akt *versus* PC12/C cells (Student's t test, two-tailed). *B*, the kinetics of cell death was analyzed in differentiated PC12/C (*solid square*), PC12/Bcl-2 (*solid diamond*), and PC12/Akt (*solid circle*) cells following deprivation of NGF/Bt_2cAMP for up to 48 h. The cells were stained with 1 μg/ml Hoechst 33258, and the apoptotic nuclei were quantified. The results are expressed as % mean ± S.E. of three independent experiments. **, $p < 0.01$; PC12/Bcl-2 or Akt *versus* PC12/C cells (Student's t test, two-tailed).

inhibit and delay the otherwise rapid translocation of hcC observed in control PC12 cells.

Immunocytochemical staining for hcC corroborated the above immunoblot analysis. PC12 control (PC12/C), PC12/Bcl-2, and PC12/Akt cells in the presence of serum showed punctate mitochondrial hcC staining evident as a rim around the nucleus. In contrast, serum deprivation of PC12/C for as little as 8 h resulted in many cells showing diffuse cytosolic hcC labeling that persisted throughout the period of serum deprivation. PC12/Bcl-2 and PC12/Akt cells deprived of serum for 8 h retained a punctate mitochondrial hcC distribution, which nonetheless became diffuse and cytosolic after 24-h deprivation (data not shown).

Cytochrome c Release in Differentiated PC12 Cells following Withdrawal of NGF/Bt_2cAMP—Like their undifferentiated counterparts, differentiated PC12 cells deprived of NGF and Bt_2cAMP also showed cytosolic hcC, which was evident by 4 h of deprivation, and persisted to 48 h (Fig. 2*A*, *panel i*), in contrast cytochrome oxidase IV was observed only within the membrane fraction (Fig. 2*A*, *panel ii*). Again, the release of hcC precedes cell death (Fig. 2*B*). Release of hcC from mitochondria was confirmed by immunocytochemical staining of equivalent cells, which showed that control differentiated PC12 cells retained punctate somatic and neuritic staining, whereas diffuse hcC staining was already evident in some cells by 4–6 h following deprivation of NGF/Bt_2cAMP. By 24 h of factor deprivation, many cells displayed both diffuse hcC cytoplasmic pattern and nuclear morphology characteristic of apoptosis (data not shown).

In undifferentiated PC12 cells, as described above, both Bcl-2 and Akt delayed hcC translocation to cytoplasm for ~18 h. No significant increase in cytosolic hcC was observed until 48 h in either differentiated PC12/Bcl-2 or PC12/Akt cells deprived of NGF/Bt_2cAMP (Fig. 2*A*, *panel iii*). 48 h after withdrawal of NGF/Bt_2cAMP, about 20% of cell death was observed in these cells (Fig. 2*B*). Immunocytochemical analysis revealed a punctate mitochondrial distribution of hcC in cell soma and neurites in 24 h factor-deprived cells that was similar to that in undeprived control cells (data not shown). Overall these results indicate that expression of either Bcl-2 or Akt in factor-deprived differentiated PC12 cells suppresses hcC release and this for a longer period than in factor-deprived undifferentiated cells.

Undifferentiated and Differentiated PC12 Cells Display Different Sensitivities to Microinjected Cytochrome c—Release of hcC implies a role of caspase 9 (and caspase 3) pathway during trophic factor deprivation. To clarify any role increased cytosolic hcC might have in PC12 cell death, undifferentiated (proliferating) and differentiated PC12 cells were each microinjected with holocytochrome *c* together with dextran-conjugated rhodamine as a fluorescent marker. In parallel experiments, the same number of cells was microinjected with dextran-rhodamine marker alone as a control for trauma from microinjections. Subsequent cell fate was then followed after various times by fluorescence microscopy. In both undifferentiated and differentiated PC12 cells, apoptosis was induced, and its extent, dependent on the dose of cytochrome *c*. However, undifferentiated cells were far more sensitive to induction of apoptosis by a given dose of microinjected cytochrome *c*. Thus, at 2 h, 40% of the injected undifferentiated cells (10 μM cytochrome *c*) had died, whereas there was no significant increase in the percentage of cell death in the differentiated population. However, by

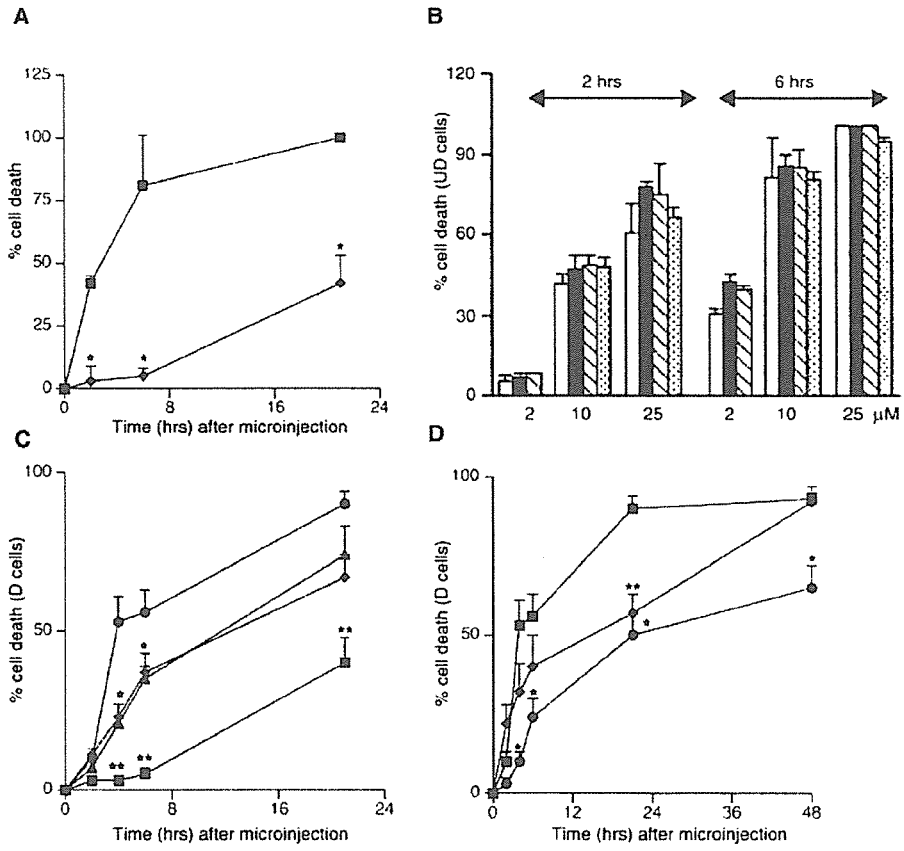

FIG. 3. **Cell death in undifferentiated and differentiated PC12 cells following cytochrome *c* microinjection.** *A*, differentiation-dependent sensitivity to microinjected cytochrome *c* (10 μM) in undifferentiated, serum-containing PC12 cells (*solid square*) and in NGF/Bt_2cAMP-differentiated PC12 cells (*solid diamond*). Cell death was quantified by counting rhodamine-positive viable and apoptotic cells at the times indicated. The results are presented as mean ± S.E. (n = 3 for undifferentiated cells and 6 for differentiated cells). *, $p < 0.05$; differentiated *versus* undifferentiated cells. *B*, different concentrations of cytochrome *c* (indicated at the *bottom*) were microinjected in undifferentiated PC12/C (*open square*), PC12/Bcl-2 (*solid square*), PC12/Akt (*square* with *bar*), or PC12/C cells treated for 24 h with NGF (100 ng/ml) (*square* with *dots*). Cell death was quantified 2 and 6 h after microinjections. The results represent mean ± S.E. of three experiments done in duplicates. *C*, the consequences of 10 μM cytochrome *c* microinjection on cell death were assessed in differentiated (*D*) PC12/C cells, either in the presence of NGF/Bt_2cAMP (*solid square*) or in the absence of NGF/Bt_2cAMP (*solid circle*). In parallel, differentiated PC12 cells deprived of NGF/Bt_2cAMP were also microinjected with rhodamine only, as control for microinjection-induced cell death (*solid diamond*). NGF/Bt_2cAMP-differentiated PC12 cells were pre-treated with benzyloxycarbonyl-VAD-fluoromethyl ketone (10 μM) for 4 h prior to cytochrome *c* microinjections (*solid triangle*). After microinjections, cell death was quantified at the times indicated by fluorescence microscopy. The results are presented as mean ± S.E. of four to six experiments. *, $p < 0.005$; cytochrome *c*-microinjected death in NGF/Bt_2cAMP-deprived cells at 4 and 6 h in cells in benzyloxycarbonyl-VAD-treated *versus* NGF/Bt_2cAMP-deprived non-treated cells. **, $p < 0.05$; cytochrome *c*-microinjected death in NGF/Bt_2cAMP-containing cells at 4, 6, and 21 h *versus* cell death in NGF/Bt_2cAMP-deprived cells (Student's *t* test, two-tailed). *D*, protection by Bcl-2 and Akt in differentiated (*D*) PC12/Bcl-2 (*solid circle*) and PC12/Akt cells (*solid diamond*) deprived of NGF/Bt_2cAMP and microinjected with 10 μM cytochrome *c*. Results of PC12/C (*solid square*) are also shown. Cell death was analyzed at different time points after microinjections, up to 48 h. The results are presented as mean ± S.E. of three to five experiments. *, $p < 0.05$, in cytochrome *c*-microinjected PC12/Bcl-2 cells *versus* PC12/C cells at 4, 6, 21, and 48 h. *, $p < 0.05$; in cytochrome *c*-microinjected PC12/Akt *versus* PC12/C cells at 21 h (Student's *t* test, two-tailed).

21 h, some 42% of microinjected differentiated PC12 cells had died, indicating that cytochrome *c* was eventually pro-apoptotic, albeit with greatly delayed kinetics (Fig. 3*A*). This differential sensitivity to microinjected hcC was also observed in cells microinjected with the higher concentration (25 μM) of cytochrome *c*, although with more rapid cell death kinetics in both undifferentiated and differentiated cells (data not shown), confirming that cytochrome *c*-induced cell death is dose-dependent. These data are consistent with the notion that differentiated PC12 cells, unlike their undifferentiated counterparts, can to some extent be protected by intracellular signals capable of ameliorating cell survival even in the presence of exogenous cytochrome *c*.

We next analyzed whether NGF, Bcl-2, or Akt inhibit cell death induced by microinjected holocytochrome c in either undifferentiated or differentiated PC12 cells. Interestingly, in undifferentiated PC12 cells, none of these factors exerted any measurable inhibitory effect on cell death kinetics analyzed 2 and 6 h following microinjections of 2, 10, and 25 μM concentrations of cytochrome *c* (Fig. 3*B*). In contrast, in differentiated PC12 cells, cell death induced by microinjection of 10 μM cytochrome *c* was significantly ameliorated by NGF/Bt_2cAMP: for example, 42 ± 10% NGF/Bt_2cAMP-treated cells died compared with 91 ± 4% dead cells in similarly microinjected cells deprived of NGF/Bt_2cAMP (Fig. 3*C*). Although withdrawal of NGF/Bt_2cAMP from differentiated PC12 cells alone leads to some cell death, this is significantly less than that observed following microinjection of cytochrome *c* (23 ± 2% control cells dead at 4 h *versus* 54 ± 8% cells microinjected with cytochrome *c*). These data indicate that increasing cytosolic cytochrome *c* in the absence of survival factors accelerates cell death in differentiated cells (Fig. 3*C*). Pre-treatment of trophic-deprived cells with the broad-specificity caspase inhibitor, benzyloxycarbonyl-VAD-fluoromethyl ketone (10 μM) inhibited, although not completely, apoptosis induced by cytochrome *c* microinjections (Fig. 3*C*), in accordance with previous reports that caspases act downstream in cytochrome *c*-mediated cell death. In sharp contrast to undifferentiated cells, we observed that

Bcl-2 and Akt suppressed cell death in differentiated PC12 cells that were deprived of NGF/Bt_2cAMP and immediately microinjected with 10 μM cytochrome *c* (Fig. 3*D*). Taken together, our results show first that sensitivity to cytosolic cytochrome *c* decreases during PC12 cell differentiation and second that in differentiated but not undifferentiated PC12 cells, Akt and Bcl-2 can suppress apoptosis downstream of cytosolic hcC.

Caspase 9 Activation Is Also Differentially Regulated between Undifferentiated and Differentiated PC12 Cells—One potential implication of our findings is that NGF/Bt_2cAMP signaling regulates cell death downstream of cytochrome *c* release, possibly at the level of activation of caspase 9. To investigate this, we next examined the abilities of extracts derived from factor-deprived PC12 cells to induce cleavage and activation of *in vitro* translated procaspase 9. Procaspase 9 is cleaved into a detectable large subunit of either 35 or 37 kDa depending on the cleavage site Asp-315 or Asp-330. Processing at Asp-330 resulting in the p37 fragment is also triggered by activated caspase 3 (31).

Incubation of cytoplasmic extracts without cytochrome *c* and dATP does not result in the autocatalytic activity of procaspase 9 (Fig. 4*A*, compare *panels a* and *b*). Only cytoplasmic extracts (soluble fraction) and not microsomal fractions prepared from trophic factor-deprived PC12 cells triggered cleavage of procaspase 9 with concomitant appearance of the signature 37- and 35-kDa large caspase 9 fragments (Fig. 4*A*, *panel c*).

No procaspase 9 cleavage was induced, in the presence of exogenous cytochrome *c*/dATP, by cytosolic extracts from NGF/Bt_2cAMP-differentiated cells maintained in NGF/Bt_2cAMP: in contrast, analogous extracts derived from differentiated PC12 cells deprived of NGF/Bt_2cAMP for 24 h triggered cleavage of the majority of procaspase 9 (Fig. 4*B*). Pre-treatment of apoptotic lysates of cells with caspase 3 inhibitor Acetyl-Asp-Glu-Val-Asp-aldehyde (Ac-DEVD-CHO) completely blocked *in vitro* processing of procaspase 9 (Fig. 4, *B* and *C*). Thus, processing of procaspase 9 is specific for cytosolic extracts from factor-deprived cells and requires DEVD-specific caspase activity. Because expression of either Bcl-2 or activated Akt suppresses apoptosis in cytochrome *c*-microinjected differentiated PC12 cells, we asked whether extracts from such cells are able to induce procaspase 9 cleavage. Indeed, as shown in Fig. 4*B*, cell extracts from factor-deprived PC12 cells expressing either Bcl-2 or activated Akt, with added cytochrome *c*/dATP exhibited no procaspase 9 cleaving activity, suggesting that Bcl-2 and Akt expression also causes modification of caspase 9 activity of these extracts.

Procaspase 9 was also not processed in the presence of cytoplasmic extracts prepared from proliferating undifferentiated PC12 cells, following addition of cytochrome *c*/dATP, but was rapidly processed by extracts from serum-deprived cells (Fig. 4*C*). Furthermore, extracts from serum-deprived PC12 cells expressing either Bcl-2 or activated-Akt were equally effective at triggering procaspase 9 processing, indicating that these factors are not exercising controls on procaspase 9 cleavage to inhibit cell death.

To confirm the critical role for caspase 9 in determining death of PC12 cells, first the processing of endogenous procaspase 9, during the withdrawal of trophic support, was verified both in undifferentiated and differentiated cells. The 37-kDa cleavage product of procaspase 9 was seen only in trophic-deprived lysates strongly indicating its potential role in cell death (Fig. 4, *D* and *E*). Because processing of caspase 9 may not necessarily signify that it is catalytically active (34), we transfected PC12 cells with a cDNA encoding a dominant negative procaspase 9 (C9DN) that has a mutation in its active site (C287S) and has been shown to block cell death (35). PC12 cells stably expressing C9DN were prepared, and the kinetics of apoptosis in both undifferentiated and NGF/Bt_2cAMP-differentiated cells was examined. Cell death induced by serum deprivation for 24 h was significantly inhibited in undifferentiated PC12/C9DN cells compared with controls (Fig. 4*F*). In addition, apoptosis of differentiated PC12 cells expressing C9DN and deprived of NGF/Bt_2cAMP for 24 h was significantly retarded (Fig. 4*G*) indicating the importance of caspase 9 for this process.

Smac/DIABLO and Omi/HtrA2 Are Also Released from Mitochondria of PC12 Cells Deprived of Trophic Support—Recent biochemical and structural studies have revealed not only how some IAP family members inhibit proteolytic activities of initiator (caspase 9) and effector caspases (caspase 3 and 7) but also the mechanism by which this inhibition is effectively eliminated during cell death by mitochondrial proteins such as Smac/DIABLO and Omi/HtrA2 (34, 36). Through their BIR (baculoviral IAP repeat) domains, IAPs bind and inhibit the catalytic activity of processed forms caspases 9, 3, and 7. The mature forms of Smac/DIABLO and Omi/HtrA2, containing an exposed IAP binding motif (IBM), once released from mitochondria promote apoptosis by binding to IAPs and relieving caspase inhibition. To determine whether the differential sensitivity to cytochrome *c* that we observe between undifferentiated and differentiated cells could be related to the mechanism of IAP regulation of caspases, we first examined the release of Smac/DIABLO and Omi/HtrA2 from mitochondria. Withdrawal of serum or NGF/Bt_2cAMP from control undifferentiated or differentiated PC12 cells, respectively, resulted in increased cytosolic levels of Smac/DIABLO and Omi/HtrA2, with kinetics similar to hcC release (Fig. 5, *A*, *panel i*, *B*, *panel i*, and *C*, *panels i* and *ii*). The effect of Bcl-2 and Akt on translocation of Smac/DIABLO in factor-deprived cells was also analyzed. Deprivation of serum in undifferentiated PC12/Bcl-2 and PC12/Akt cells resulted in delayed cytoplasmic accumulation of Smac/DIABLO (at around 18 h) (Fig. 5*A*, *panels ii* and *iii*), although the results of quantification showed that, like hcC, the amount released at 18 h was less than that seen in control cells. In contrast, in NGF/Bt_2cAMP-deprived PC12/Bcl-2 or PC12/Akt-differentiated cells, cytoplasmic accumulation of these proteins was not observed even at 24 h (Fig. 5*B*, *panels ii* and *iii*). These results suggest that Bcl-2 and Akt co-regulate the release of hcC together with other pro-apoptotic factors from mitochondria during withdrawal of trophic support.

Differentiated but Not Undifferentiated PC12 Cells Are Sensitive to Active Smac/DIABLO—Proteolytic processing of Smac/DIABLO or Omi/HtrA2 results in the removal of mitochondrial signal peptide sequence and exposure of a novel N termini or IBM containing the tetrapeptide sequence AVPI, which has been shown to bind to IAPs (37, 38). To elucidate whether cytochrome *c* sensitivity of caspase 9 pathway is dependent on AVPI proteins, undifferentiated and differentiated PC12 cells were transiently co-transfected with plasmids encoding cDNAs for GFP and ubiquitin (Ub) fused to ΔN-AVPI Smac/DIABLO or the inactive Ub-ΔN-MVPI Smac/DIABLO. Intracellular processing of ubiquitin has been shown to yield mature Smac/DIABLO protein with exposed tetrapeptide sequence (39). Cell death was monitored and quantified by counting Hoescht stained apoptotic nuclei of GFP-positive cells, at 8 and 24 h following withdrawal of trophic support. In undifferentiated PC12/C cells, following withdrawal of serum, increased cell death was observed at 8 and 24 h; however, there was no difference in cultures transfected with Ub-ΔN-AVPI or MVPI-smac/DIABLO. There was some cell death at 8 h in control cells, which may be due to other regions than N-terminal of Smac/DIABLO-sensitizing serum-deprived cells to apoptosis (40) (Fig. 6*A*). Transfection of Ub-ΔN-AVPI-smac/DIABLO in

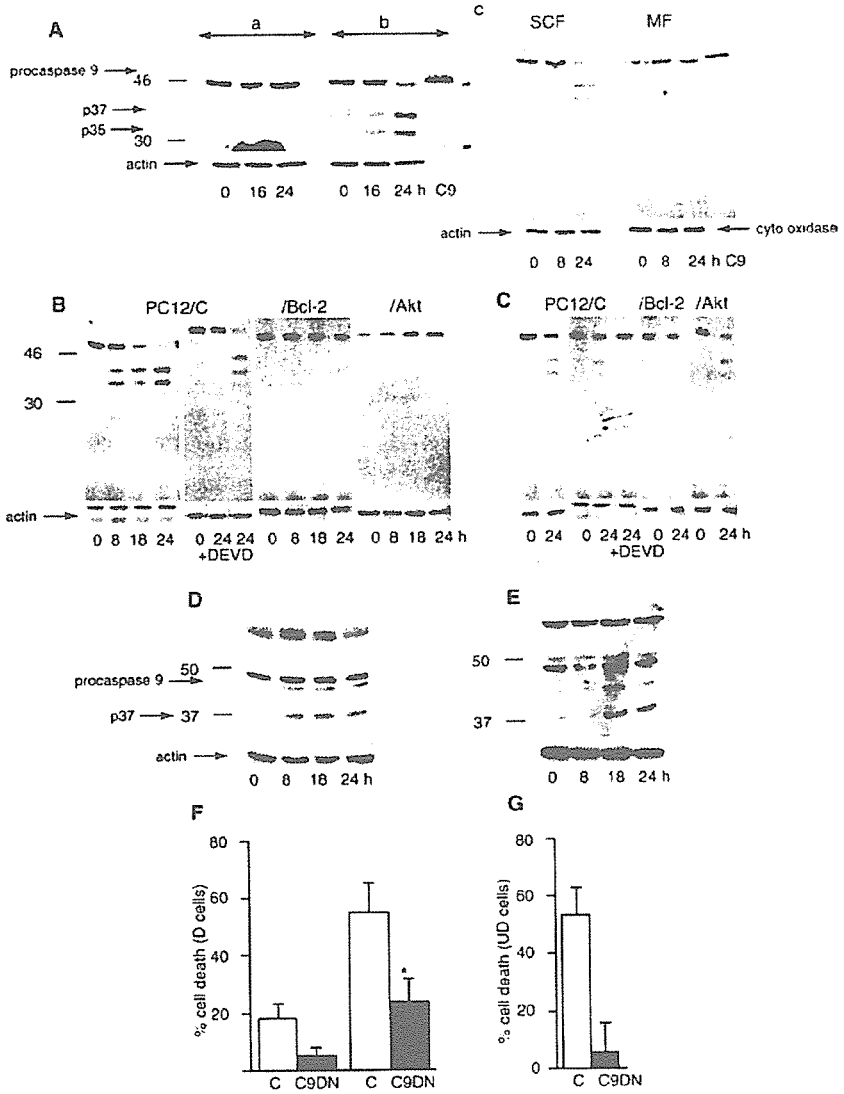

FIG. 4. **Regulation and role of caspase 9 in cell death of trophic support deprived PC12 cells.** *A*, ^{35}S-labeled procaspase 9 processing by cytosolic extracts prepared from differentiated PC12 cells deprived of NGF/Bt_2cAMP for 16 and 24 h in the absence (*a*) and presence (*b*) of 10 mM cytochrome *c* and 1 mM dATP. Processing of *in vitro* labeled procaspase 9 was analyzed in membrane (*MF*) and in soluble cytosolic fractions (*SCF*) in the presence of cytochrome *c*/dATP (*c*). An aliquot (1.5 μl) of *in vitro* translated procaspase 9 product is shown in the last lane (*C9*). Shown also are the results of actin and cytochrome oxidase as protein controls of the SCF and MF lysates, respectively, used in the reaction. These controls were done separately using the same lysates and the same amount of total protein (20 μg). *B*, kinetics of procaspase 9 processing in differentiated PC12/C cells deprived of NGF/Bt_2cAMP. Cytoplasmic lysates were prepared at times indicated after withdrawal of NGF/Bt_2cAMP. Addition of caspase inhibitor Ac-DEVD-CHO inhibits procaspase 9 processing in extracts from differentiated PC12/C cells deprived of NGF/Bt_2cAMP for 24 h. Procaspase 9 is not processed in lysates prepared from differentiated PC12/Bcl-2 cells or PC12/Akt cells. NGF/Bt_2cAMP was withdrawn from these cells at times indicated. Results of actin as control for lysates used are shown below. *C*, procaspase 9 processing in undifferentiated PC12 cells containing serum (0) and following serum deprivation for 24 h that stimulates the processing, which was not prevented in PC12/Bcl-2 or PC12/Akt cells. However, prior Ac-DEVD-CHO treatment inhibited caspase 9 processing. Actin control is shown below. *D* and *E*, endogenous cleavage of caspase 9 following withdrawal of trophic support from differentiated (*D*) and undifferentiated (*E*) cells. The anti-caspase 9 antibody recognized procaspase 9 and the p37 large subunit, which is evident in trophic factor-deprived lysates. The bots were probed with anti-actin antibody as control for protein loading. *F* and *G*, inhibition of cell death in PC12 cells expressing dominant negative caspase 9 (*PC12/C9DN*). Cell death, in the presence of trophic support, time 0 h, in undifferentiated and differentiated cells in PC12/C and PC12/caspase 9 DN is 4–5 ± 2% (mean ± S.E.). *F*, differentiated (*D*) PC12/C and PC12/C9DN were deprived of NGF/Bt_2cAMP for 16 and 21 h (n = 4). Apoptotic cells were quantified after staining with 1 μg/ml Hoechst 33258. *, $p < 0.05$; cell death in control *versus* in C9 dominant negative cells. *G*, undifferentiated (*UD*) cells were deprived of serum for 24 h. The results are presented as mean ± S.D. (n = 3).

factor-deprived undifferentiated PC12/Bcl-2 or PC12/Akt cells did not result in significantly more cell death compared with cells transfected with Ub-ΔN-MVPI Smac/DIABLO (Fig. 6*A*). In contrast, NGF/Bt_2cAMP-deprived control, Bcl-2-expressing, or Akt-expressing differentiated PC12 cells were susceptible to cell death by Ub-ΔN-AVPI Smac/DIABLO but not Ub-ΔN-MVPI Smac/DIABLO (Fig. 6*B*). Increased cell death in PC12/C-differentiated cells was seen even in the presence of NGF/Bt_2cAMP. These results suggest that, although IBM of Smac/DIABLO is not required for cell death by trophic factor deprivation in undifferentiated cells, it plays an important role in regulating caspase activation in differentiated cells. Further, the anti-apoptotic function of Bcl-2 and Akt is antagonized by Ub-ΔN-AVPI Smac/DIABLO in differentiated cells indicating that inhibition of Smac/DIABLO release by Bcl-2 or Akt is crucial to suppressing cell death.

Role of IAPs in Regulating Cell Death in Undifferentiated and Differentiated PC12 Cells—The above results strongly indicate that the release of mitochondrial proteins Smac/DIABLO and Omi/HtrA2 that act to relieve IAP inhibition of

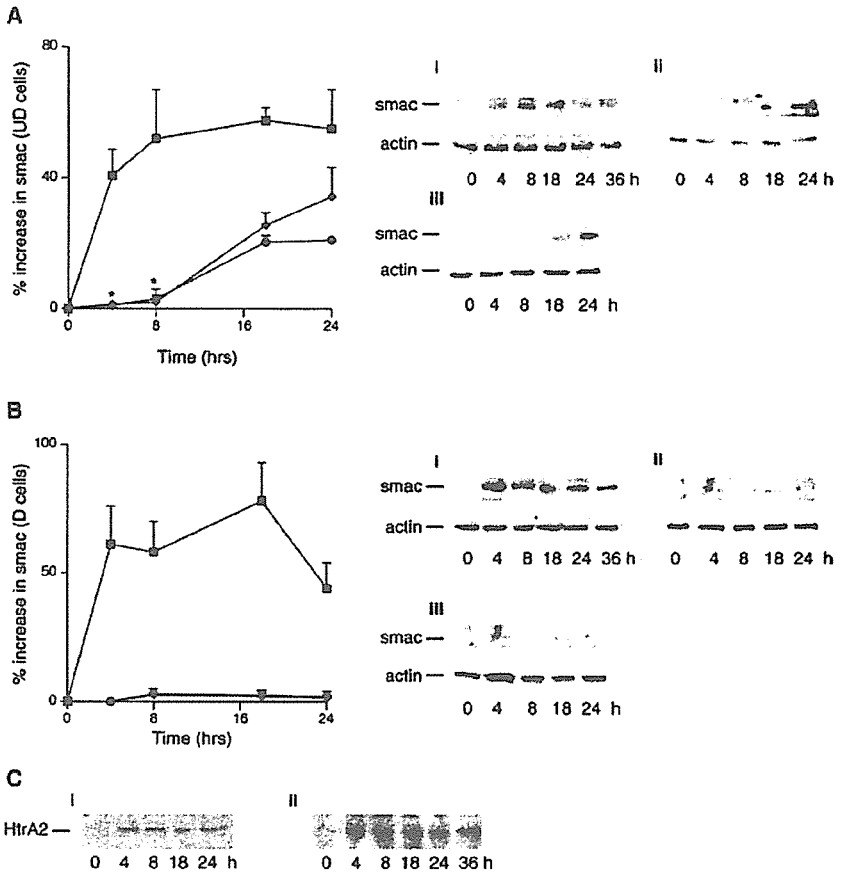

FIG. 5. **Immunoblot analysis of Smac/DIABLO and omi/HtrA2 levels in undifferentiated and NGF/Bt_2cAMP-differentiated PC12 cells following trophic factor deprivation.** *A*, for immunoblot analysis of Smac/DIABLO in undifferentiated (*UD*) cells, 20 μg of total protein of SCF was used, and the blots were probed with anti-smac antibody. Shown are representative results of Smac in: *i*, PC12/C cells containing serum (0) deprived of serum for times indicated (h); *ii*, undifferentiated PC12/Bcl-2; and *iii*, PC12/Akt cells deprived of serum. Results of actin are shown as control for loading. The autoradiograms were quantified and % increase in cytosolic Smac was calculated using the intensity value at 0 h as control. The results are expressed as mean ± S.E. (n = 3–4). *, $p < 0.05$ PC12/Bcl-2 and Akt *versus* PC12/C cells. *B*, Smac levels in differentiated PC12 cells (0) deprived of NGF/Bt_2cAMP at times indicated (h). Shown are representative results of Smac in SCF in: *i*, PC12/C cells; *ii*, PC12/Bcl-2 cells; and *iii*, PC12/Akt cells. Quantification of autoradiograms are represented as % increase (mean ± S.E., n = 3–4) in Smac in cytosolic fraction. *C*, 30 μg of total protein of SCF was used for HtrA2/Omi analysis in trophic-deprived undifferentiated (*i*) and differentiated (*ii*) PC12/C for the times indicated.

caspase 9 cascade, is an important determinant of cytochrome *c* sensitivity in undifferentiated and differentiated cells. To ascertain the role of differentiation, we first examined for changes in levels of c-IAP-2 and XIAP as well as Smac/DIABLO andOmi/HtrA2 in undifferentiated *versus* differentiated cells (Fig. 7*A*). Quantification of the results using actin as control in each case showed that the levels of XIAP, Smac/DIABLO, and Omi/HtrA2 remain the same, however there is 41 ± 3% (n = 3) increase in c-IAP-2 levels in differentiated cells. Next we analyzed the levels of XIAP and c-IAP-2 during deprivation of trophic support. In undifferentiated PC12/C, Bcl-2, or Akt cells, XIAP protein levels were unaltered following withdrawal of serum (Fig. 7*B*). In contrast, in PC12/C-differentiated cells, withdrawal of NGF/Bt_2cAMP resulted in decreased level of XIAP at 24 h (25–35%) (Fig. 7*C*). This change in XIAP protein level was not seen in differentiated PC12/Akt or PC12/Bcl-2 cells following deprivation of NGF/Bt_2cAMP (Fig. 7*C*). In contrast to XIAP, there were no changes in c-IAP-2 levels (data not shown). Taken together with the above AVPI data, these results suggest that XIAP and c-IAP-2 play a role in regulating caspase 9 cascade in differentiated but not undifferentiated cells. To further examine this possibility, we constructed an inducible XIAP-tetracycline-repressible PC12 cell line to examine whether sensitivity to microinjected cytochrome *c* decreases in undifferentiated cells. Undifferentiated PC12 cells in the presence or absence of doxycycline were microinjected with 2, 10, and 25 μM cytochrome *c*, and cell death was quantified after 6 h (Fig. 7*D*). In sharp contrast to results obtained with PC12/C, PC12/Bcl-2, and PC12/Akt cells (*cf.* Fig. 3, *A* and *B*), these cells were resistant to microinjected cytochrome *c*. However, in the presence of doxycycline these cells were not as sensitive to microinjected cytochrome *c* as PC12/C cells (*cf.* Fig. 3, *A* and *B*). The highest concentration of doxycycline that these cells could tolerate was 0.5 μg/ml, which may not completely repress tetracycline. The results of immunoblot analysis of XIAP in the absence and presence indicate that XIAP levels are higher in doxycycline-treated cells (Fig. 7*D*). Nevertheless, inhibition of cell death was greater in cells in which doxycycline was withdrawn. Quantification of cell death upon deprivation of trophic support for 24 h in both undifferentiated and differentiated cells showed cell death that is less efficient in the absence than in presence of doxycycline (Fig. 7*E*). In PC12/XIAP cells, cell death in the presence of doxycycline was less compared with PC12/C cells (*cf.* Figs. 1*B* and 2*B*). Overall the results indicate that both XIAP and c-IAP-2 regulate caspase 9 and possibly caspases 7 and 3 activation in differentiated cells.

DISCUSSION

The characteristics of PC12 cells make them a useful and tractable *in vitro* model with which to examine the parameters regulating cell survival in both proliferating neuroectoderm-derived neoplastic cells and in differentiated neuronal cells. In this study, we have shown that hcC, Smac/DIABLO, and Omi/HtrA2 are released from the mitochondrial compartment of factor-deprived PC12 cells undergoing apoptosis. Moreover, ectopic expression of a dominant interfering mutant of caspase 9 inhibits such cell death. Thus, the mitochondrial hcC-caspase 9-cell death pathway is both activated and important in determining cell death of factor-deprived PC12 cells. We also investigated the regulation exerted by Bcl-2 and activated-Akt on hcC and Smac/DIABLO release from mitochondria and the induction of cell death by cytosolic hcC and caspase 9 activation. We find that in both undifferentiated and differentiated (post-mitotic) PC12 cells, Bcl-2 and Akt exert a suppressive effect on release of hcC and Smac/DIABLO, the effect persisting longer in differentiated cells. Moreover, in contrast to un-